Special Publication 19, pp. 29–55

Chapter 2

Magmatic and Metallogenic Framework of Au-Cu Porphyry and Polymetallic Carbonate-Hosted Replacement Deposits of the Kassandra Mining District, Northern Greece*

Chris R. Siron,[1,†] John F.H. Thompson,[1] Tim Baker,[2] Richard Friedman,[3] Pavlos Tsitsanis,[4] Sally Russell,[4] Scott Randall,[4] and Jim Mortensen[3]

[1] *Department of Earth and Atmospheric Sciences, Cornell University, Ithaca, New York 14853*

[2] *Eldorado Gold Corporation, 1188 Bentall 5-550 Burrard St., Vancouver, British Columbia, Canada V6C 2B5*

[3] *Pacific Center for Isotopic and Geochemical Research, 2207 Main Mall, University of British Columbia, Vancouver, British Columbia, Canada V6T 1Z4*

[4] *Eldorado Gold Exploration, 23a Vassilissis Sofias Ave., 106 74, Athens, Greece*

Abstract

The Kassandra mining district in the eastern Chalkidiki Peninsula of northern Greece contains ~12 Moz Au in porphyry and polymetallic carbonate-hosted replacement sulfide orebodies. Zircon U-Pb geochronology defines two distinct magmatic episodes in the late Oligocene (27–25 Ma) and early Miocene (20–19 Ma). Both suites are characterized by high K calc-alkaline magmas with the younger early Miocene porphyritic stocks and dikes having indications of shoshonitic geochemistry. Normalized rare earth element patterns support plagioclase fractionation among the late Oligocene suite, whereas amphibole or garnet fractionation is more likely for early Miocene porphyries.

Carbonate replacement mineralization is hosted in marble contained within the semibrittle Stratoni fault zone. Mineralization varies along the 12-km strike length of the fault zone from Cu-bearing skarn adjacent to the late Oligocene Stratoni granodiorite stock westward into Au-Ag-Pb-Zn-Cu carbonate replacement deposits at Madem Lakkos and Mavres Petres. Piavitsa, at the western end of the exposed fault zone, hosts siliceous Mn-rich replacement bodies associated with crustiform Au-rich quartz-rhodochrosite veins. Structural and alteration relationships suggest that carbonate replacement mineralization is syn- to postemplacement of the late Oligocene Stratoni granodiorite stock at 25.4 ± 0.2 Ma. The Olympias Au-Ag-Pb-Zn carbonate replacement deposit, located north of the Stratoni fault zone, is hosted in marble and associated semibrittle structures. Olympias is broadly similar to the Madem Lakkos and Mavres Petres deposits. Early Miocene Au-Cu mineralization at Skouries is associated with a narrow pipe-shaped multiphase porphyry stock emplaced into the hinge zone of a regional antiform.

Late Oligocene and early Miocene magmatism overlaps spatially within the district but defines distinct petrogenetic events separated by about 5 m.y. Carbonate replacement massive sulfide deposition was largely controlled by an extensional structure and receptive host rocks within the fault zone, whereas a major regional fold axis localized the Skouries porphyry system. The change in character of mineralization with time may reflect a combination of factors including preexisting structural control, magmatic-hydrothermal processes, and the availability of reactive host rocks.

Introduction

The Kassandra mining district is located on the eastern Chalkidiki Peninsula approximately 100 km east of Thessaloniki. The cumulative gold endowment, ~12 million ounces (Moz) Au (Eldorado Gold Corp., 2016) in porphyry and carbonate-hosted replacement-style sulfide orebodies, makes this district one of the most economically significant mining camps in the Serbo-Macedonian metallogenic province (Hahn et al., 2012). Polymetallic orebodies occur at Olympias, Madem Lakkos, and Mavres Petres, and Au-Cu mineralization is hosted by the Skouries porphyry. Olympias contains a measured resource of 16.3 million metric tons (Mt) at 8.6 g/t Au, 146 g/t Ag, 4.9% Pb, and 6.5% Zn (Eldorado Gold Corp., 2016), including 1.86 Mt grading 3.4 g/t Au in economically recoverable stockpiles from previous operations. Past mining at Madem Lakkos produced approximately 13.5 Mt of Ag-Pb-Zn ore (Forward et al., 2010). Mavres Petres has a measured resource of 1.1 Mt at 210 g/t Ag, 7.9% Pb, and 10.5% Zn (Eldorado Gold Corp., 2016). The Skouries Au-Cu porphyry contains a measured and indicated resource of 283.6 Mt grading 0.6 g/t Au and 0.43% Cu (Eldorado Gold Corp., 2016).

Mining of gold and silver ores in the Chalkidiki region dates from antiquity, about 350 B.C., during the rule of King Phillip II of Macedon and his successor, Alexander the Great. Historic records indicate that the extraction of ores from the mines of Potidaea and Mt. Pangaeus financed expansion of the empire (e.g., Diodorus Siculus, 1963). The region experienced limited activity during Roman rule and intermittent development during the 9th and 15th centuries A.D. while under Byzantine and Ottoman occupation, respectively (Haines, 1998). Mineral extraction occurred throughout the 20th century with modern exploration and mining practices established during the 1960s and 1970s when the Hellenic Chemical Products and Fertilizers Company Ltd. operated the Madem Lakkos

† Corresponding author: e-mail, crs344@cornell.edu

* Digital Appendix Tables for this paper are available online at www.segweb.org/SP19-Appendices.

and Olympias mines, and exploration was undertaken at Skouries by Nippon Mining, Placer International, and Penaroya (Tobey et al., 1998). Billiton Resources briefly evaluated Skouries in the early 1980s (Tobey et al., 1998). TVX Gold took over mining at Madem Lakkos and Olympias in 1995, and exploration and resource evaluation continued at Olympias and Skouries through 2002. European Goldfields held the concessions prior to acquisition in 2012 by Eldorado Gold Corporation. Currently, Mavres Petres is an operating mine, tailings are being reprocessed at Olympias, and new mine development is underway at Skouries and Olympias.

The objective of this study is to describe the metallogenic framework of the Kassandra mining district based on the structural architecture of the area and the timing and petrogenesis of Oligo-Miocene magmatism. The work was based on mapping approximately 250 km², logging representative drill holes, and compilation of drill and exploration data. We present petrography, whole-rock geochemistry, and high-precision zircon U-Pb geochronology defining ages for intrusive rocks belonging to Oligo-Miocene magmatism. These results further constrain the timing of Oligo-Miocene magmatism that builds upon previous work, and improves understanding of the metallogenic evolution of Au-Cu porphyry and Au-rich polymetallic carbonate-hosted replacement deposits of the region. All data from this study including sample location information are presented in Appendices A1 and A2.

Regional Geologic Framework

The Hellenides of northern Greece form a segment of the Alpine-Himalayan mountain chain connecting the Balkan Peninsula with the Anatolides of Turkey. This section of the orogenic belt resulted from the convergence of the Apulian and Pelagonian microcontinents with the Serbo-Macedonian and Rhodope continental fragments previously accreted to the Eurasian margin during the Late Cretaceous to early Eocene (Pe-Piper and Piper, 2006). Convergence of microcontinents and subduction of oceanic lithosphere led to magmatism resulting from slab detachment or lithospheric delamination assisted by rollback of the subducting slab during post-collisional back-arc extension of the subduction wedge (de Boorder et al., 1998; Wortel and Spakman, 2000; Lips, 2002; Neubauer, 2002; Brun and Sokoutis, 2010; Ring et al., 2010; Jolivet et al., 2013; Papanikolaou, 2013).

The Rhodope metamorphic province is described as an amphibolite-grade, crustal-scale, synmetamorphic accretionary wedge consisting of stacked nappes that lie in the hinterland of the Hellenic subduction zone (Burg et al., 1990, 1996; Ricou et al., 1998; Gautier et al., 1999; Bonev et al., 2006; Krenn et al., 2010). The Greek segment of the Rhodope metamorphic province extends to the southwest to the Vardar suture zone (Ricou et al., 1998) and is bound to the northeast by the Maritza strike-slip fault and the Thrace basin. Kydonakis et al. (2014) divided the Rhodope metamorphic province into three tectonic domains: northern Rhodope complex, southern Rhodope metamorphic core complex, and the Serbo-Macedonian domain. In the Chalkidiki region, the Serbo-Macedonian Vertiskos unit is separated from the southern Rhodope metamorphic core complex by the Kerdilion detachment fault (Fig. 1; Brun and Sokoutis, 2007; Wüthrich, 2009; Kydonakis et al., 2014).

The Vertiskos unit is a Silurian-age exotic terrane that belonged to a continental magmatic arc of Gondwana origin that was accreted onto the European margin in the Carboniferous (Himmerkus et al., 2006, 2007, 2009a). The Vertiskos unit consists of leucocratic augen gneisses and kyanite- and staurolite-bearing schist (Himmerkus et al., 2009a) that reached amphibolite-facies metamorphic conditions in the Late Jurassic to Early Cretaceous (Kilias et al., 1999; Lips et al., 2000). The Kerdilion unit originated from a Permo-Carboniferous magmatic arc overlain by Tethyan carbonates, and later witnessed magmatic activity during the Late Jurassic and Cretaceous (Turpaud and Reischmann, 2003; Himmerkus et al., 2011), and again during the early Miocene related to exhumation of the metamorphic dome (Jones et al., 1992; Dinter et al., 1995). Orthogneiss, paragneiss, marbles, micaceous schists, and amphibolite of the Kerdilion unit form the tectonic upper and westernmost portion of the southern Rhodope metamorphic core complex (Burg et al., 1993; Brun and Sokoutis, 2007; Himmerkus et al., 2011).

Triassic rifting of the European arc resulted in the opening of the Vardar Ocean and development of mafic units (Dixon and Dimitriadis, 1984; Himmerkus et al., 2005; Bonev and Dilek, 2010) and intrusion of A-type granites of the Arnea-Kerkini suite (Christofides et al., 2007). This magmatic event is evident in the Chalkidiki region with the Arnea granite that intruded the Vertiskos unit at 228 ± 5.6 Ma (De Wet et al., 1989; Himmerkus et al., 2009b). The Arnea suite is interpreted to have a within-plate tectonic signature characteristic of a rift-dominated environment similar to Triassic-age granites elsewhere in the Aegean (Himmerkus et al, 2009b). Closure of the Vardar Ocean during the Cretaceous Alpine orogeny culminated in amphibolite-grade metamorphism of the Serbo-Macedonian domain and the Triassic rift-related granites (Himmerkus et al., 2009b). Ductile deformation of the Kerdilion unit, however, was accompanied by early to middle Eocene upper greenschist- to lower amphibolite-grade metamorphism, with a retrograde greenschist metamorphic overprint (Wawrzenitz and Krohe, 1998; Lips et al., 2000).

The Vertiskos unit is separated from the southern Rhodope Kerdilion unit by the arcuate Athos-Volvi suture zone (Himmerkus et al., 2005) and the Kerdilion fault (Fig. 1; Kydonakis et al., 2014). Amphibolite, garnet-amphibolite, and serpentinized ultramafic rocks form a tectonic mélange with the adjacent gneisses. Mafic and ultramafic rocks belonging to the Athos-Volvi or Thermes-Volvi-Gomati ophiolite complex (Dixon and Dimitriadis, 1984; Bonev and Dilek, 2010) are classified as noncumulate and cumulate low K tholeiites of gabbroic to hartzburgitic composition (Himmerkus et al., 2011). Previous geochemical and isotopic studies indicate a within-plate signature consistent with formation in an intracontinental rift or back-arc environment within a supra-subduction zone setting (Dixon and Dimitriadis, 1984; Himmerkus et al., 2005; Bonev et al., 2012). These bodies were subsequently emplaced between the crustal blocks of the Vertiskos and Kerdilion units during the Hellenic orogeny (Himmerkus et al., 2005).

Widespread crustal extension in the northern Aegean region began in the mid-Eocene to mid-Oligocene. Approximately 120 km of extensional displacement and 30° of dextral rotation of the Chalkidiki block was imparted by exhumation of

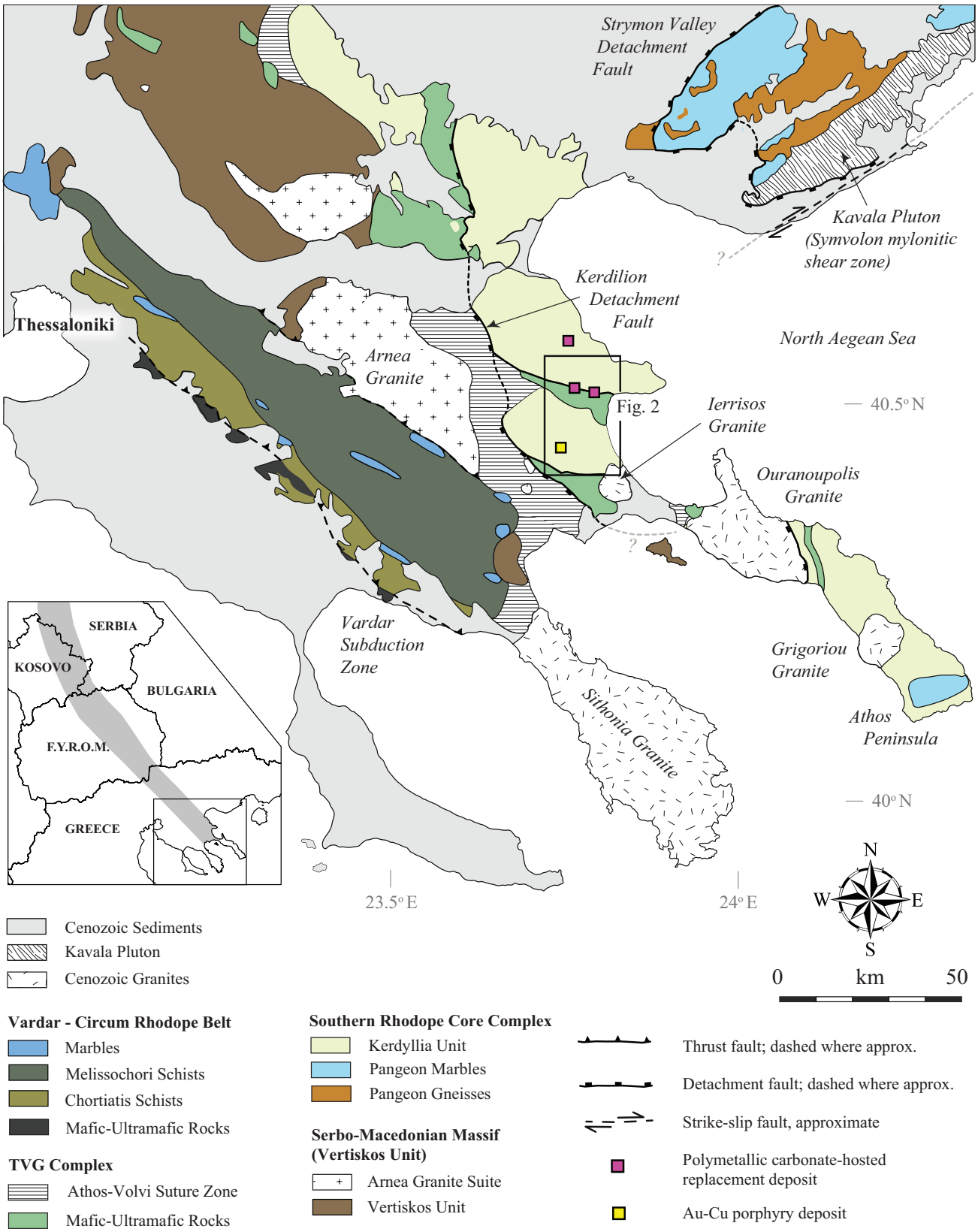

Fig. 1. Simplified geologic map of the Chalkidiki peninsula after Himmerkus et al. (2011), including the Strymon valley detachment fault adopted from Dinter (1998) and the northern segment of the Kerdilion detachment fault after Brun and Sokoutis (2007) and Wüthrich (2009). Inset map depicts the location of the Oligo-Miocene Serbo-Macedonian Lece-Chalkidiki metallogenic belt (gray) after Janković (1997) and Serafimovski (2000).

the southern Rhodope metamorphic core complex (Dimitriadis et al., 1998; Brun and Sokoutis, 2007). Extensive magmatism and widespread volcanic activity began in the Oligocene (Fytikas et al., 1984; Pe-Piper and Piper, 2002; Ring et al., 2010) in response to plate convergence and crustal extension.

District Geology

The Serbo-Macedonian metallogenic province (Janković, 1997) spans the length of the Hellenide orogen (Fig. 1). Porphyry and carbonate-hosted replacement deposits of the Kassandra mining district are hosted by the high-grade metamorphic basement rocks of the Kerdilion unit (Brun and Sokoutis, 2007). The W-dipping Kerdilion detachment fault crops out to the northwest, at the contact of the Kerdilion unit with the imbricated schists and gneiss of the Athos-Volvi suture zone (Fig. 1). This structure is interpreted to have accommodated exhumation of the southern Rhodope core complex beginning in the middle Eocene (Brun and Sokoutis, 2007; Wüthrich, 2009; Kydonakis et al., 2014). A ductile shear zone similar in structural style to the Kerdilion fault occurs within the Athos-Volvi suture zone on the Athos peninsula (Himmerkus et al., 2011) southeast of the Kassandra mining district. This ductile shear zone coalesces with the Kerdilion fault, forming a continuous tectonic boundary between the Vertiskos unit to the south and west and the Kerdilion unit to the east and north (Fig. 1).

Kerdilion unit

The Kerdilion unit is well exposed north of the Stratoni fault where it consists of migmatitic quartzo-feldspathic biotite gneiss, megacrystic plagioclase-microcline granitic gneiss, amphibolite, and marbles. The Stratoni fault is a zone of WNW-trending, S- to SW-dipping normal faults cropping out over 12 km from the village of Stratoni and west to Piavitsa (Fig. 2). The hanging wall of the Stratoni fault to the south is composed of amphibolite, potentially correlative with the Thermes-Volvi-Gomati complex of Dixon and Dimitriadis (1984), and a thick sequence of carbonaceous-biotite gneisses and schists interlayered with minor calcareous schists and marble. Kockel et al. (1977) assigned the hanging-wall lithologic sequence to the Vertiskos unit and this classification was adopted by subsequent studies in the area (e.g., Kalogeropoulos et al., 1989b; Frei, 1995). Observations from outcrop and drill core suggest a gradational contact between carbonaceous-biotite gneiss and amphibolite hanging-wall rocks to the south of the Stratoni fault with footwall quartzo-feldspathic biotite gneiss and marble to the north. Marble and amphibolite occur on both sides of the fault although marble is prevalent to the north and amphibolite is dominant to the south. Furthermore, interlayered calcareous schists and marble associated with hanging-wall gneisses are not characteristic of the Vertiskos unit and are more closely related to the Kerdilion unit (Himmerkus et al., 2011). Therefore, it is proposed that the Kerdilion unit is present on both sides of the Stratoni fault although there are lithologic changes that more or less coincide with the fault zone.

Abundant aplite and pegmatite dikes and sills of Eocene to Oligocene age occur throughout the footwall quartzo-feldspathic gneiss sequence (Kalogeropoulos et al., 1989b). Coarse-grained pegmatites and fine- to medium-grained aplites typically exhibit a discrete penetrative tectonic fabric or boudinage and are likely derived from anatectic processes during deformation (Kalogeropoulos et al., 1989b; Haines, 1998). Some of the aplitic dikes appear undeformed, suggesting that anatexis continued postdeformation.

Magmatism

The district has witnessed a protracted magmatic history from the Late Cretaceous to early Eocene (Pe-Piper and Piper, 2002). Magmatism during this period is characterized by subduction-related calc-alkaline granites exposed at Ierissos (Frei, 1992, 1996), Ouranoupolis (De Wet et al., 1989), and Grigoriou (Bébien et al., 2001), which crop out within the Athos-Volvi suture zone and Kerdilion unit (Fig. 1; Himmerkus et al., 2011). These granitic intrusions exhibit a weak tectonic fabric, suggesting emplacement at the waning stages of regional Alpine deformation. Crystallization ages range from 66.8 ± 0.8 and 68 ± 1 Ma for an unnamed intrusion outcropping near the Ouranoupolis granite (Himmerkus et al., 2011) to 53 ± 4 Ma for the Ierissos granite (Frei, 1992, 1996). The latter is similar in age to the Sithonia granite to the south (Christofides et al., 1990). Biotite and muscovite $^{40}Ar/^{39}Ar$ cooling ages from the Ouranoupolis granite are 47 ± 0.7 and 44 ± 1.1 Ma, respectively (De Wet et al., 1989). These ages are consistent with the biotite K-Ar cooling age from the Grigoriou granite of 43 ± 1 Ma (Bébien et al., 2001). Late Oligocene and early Miocene intrusions crop out along a NE-trending belt within the Kerdilion unit and are discussed in detail in subsequent sections.

Structure

The Kerdilion unit of the southern Rhodope core complex displays a regionally consistent flat-lying extensional ductile fabric with a uniform top-to-the southwest sense of shear and NE-SW-stretching lineations (Eliopoulos and Kilias, 2011). The Kerdilion unit within the Kassandra mining district similarly exhibits a penetrative shallow dipping S_1 foliation defined by alignment of peak metamorphic minerals (e.g., feldspar and amphibole). A subsequent or cotectonic high-strain event resulted in tight to isoclinal F_2 folds locally accompanied by subparallel axial planar S_2 cleavage. An ensuing lower strain deformation event superimposed a spaced and associated steeply dipping S_3 foliation, warping previously developed fabrics. This event is associated with kilometer-scale upright and open E-plunging F_3 folds evident as district-scale antiforms in the footwall of the Stratoni and Gomati faults, respectively (Fig. 2). Both folds mimic the arcuate contact of the Stratoni fault and Athos-Volvi suture zone, suggesting a geodynamic relationship.

Early movement on the Stratoni fault may have included top-to-the north ductile thrust faulting during compressional tectonism at lower amphibolite metamorphic conditions (Haines, 1998). District-scale F_3 fold kinematics are consistent with this interpretation. The transition from compression to extensional tectonics, probably in the early Oligocene, resulted in SW-dipping mylonitic ductile shear zones superimposed on the previous thrust fabrics (Haines, 1998). Subsequent late Oligocene semibrittle deformation consists of cataclastic textures with development of internal foliation and pressure solution fabrics which are overprinted by younger

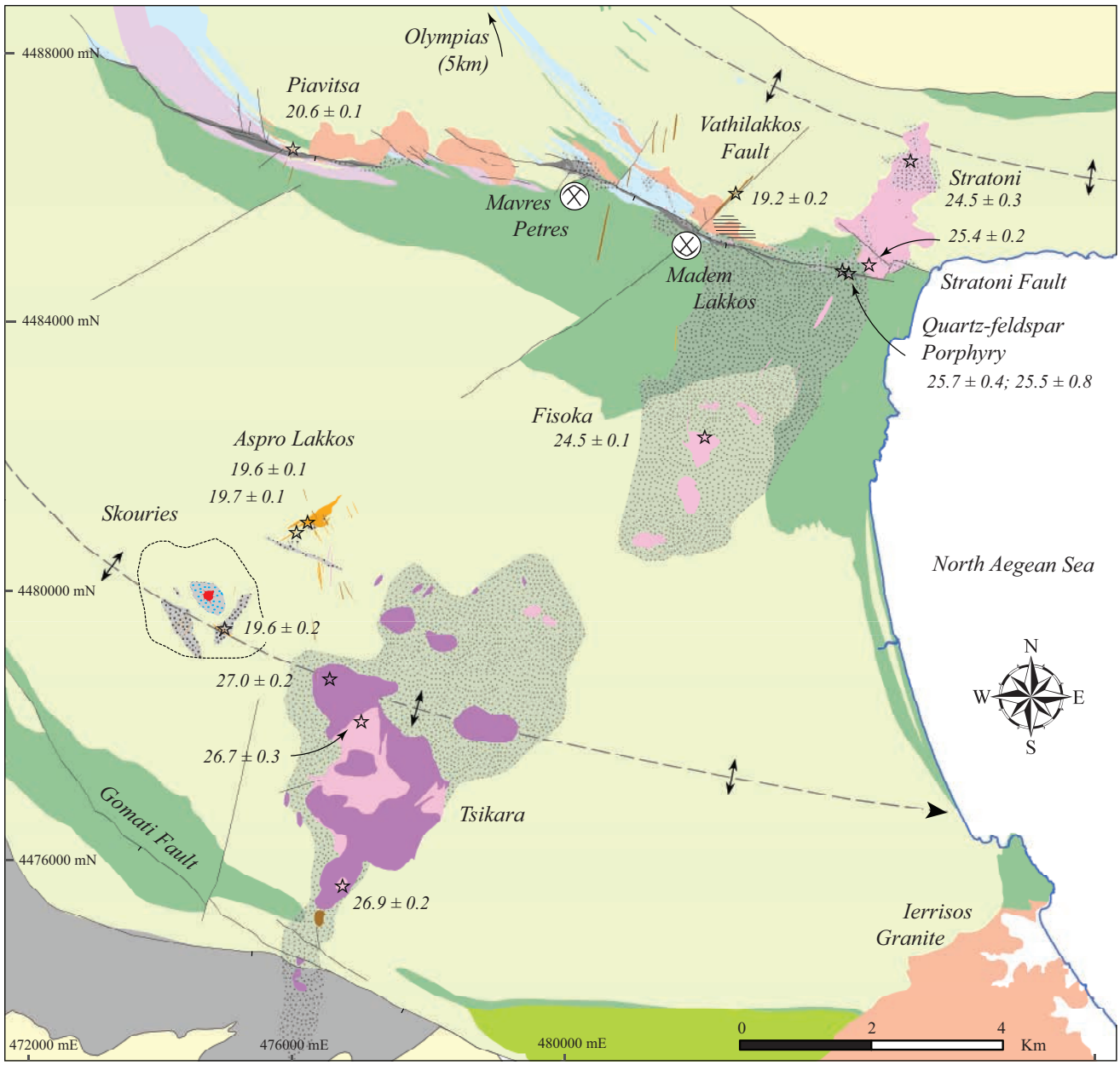

Metamorphic Basement Rocks

- Quartz-feldspar granite gneiss
- Plagioclase-microcline gneiss
- Amphibolite, metagabbro, pyroxenite with serpentinized peridotite and dunite (TVG complex)
- Quartz-feldspar-biotite gneiss
- Marble, locally graphitic
- Graphite-bearing quartz-biotite gneiss
- Leucocratic augen gneiss (Vertiskos?)

Oligo-Miocene Intrusive Rocks

- Quartz monzonite porphyry
- Glomerophyric porphyry dikes
- Quartz monzonite porphyry (Skouries)
- Granodiorite/granodiorite porphyry
- Monzogabbro and monzodiorite

Alteration

- Quartz-sericite-pyrite (QSP)
- Amphibole-magnetite-biotite (Skouries)
- Wolastonite-tremolite-epidote (skarn)

Map Symbology

- Normal fault with dip and damage zone, dashed where approx.
- Antiform with plunge direction (approx.)
- Fault
- Zircon U-Pb sample location
- Active Mine
- Closed Mine
- Demagnetization (pyrite) halo at Skouries defined by unpub. aero-magnetic data

Fig. 2. Geologic map of the Kassandra mining district modified after Kockel et al. (1975). Coordinates measured using Greek Geodetic Coordinate System (GGRS 87 Greek Grid).

phases of brittle fault gouge (Siron et al., 2014). Sulfide minerals intergrown with and overprinting the tectonic fabric support synmineral deformation. Steeply dipping NNE-trending right-lateral strike-slip faults are kinematically compatible with extension on the Stratoni fault. The Stratoni fault and the massive sulfide orebody at Madem Lakkos, however, are displaced by the NE-trending right-lateral strike-slip fault at Vathilakkos (Fig. 2; Kalogeropoulos et al., 1991; Nebel et al., 1991; Gilg and Frei, 1994; Haines, 1998), suggesting that movement on these structures persisted after major movement on the Stratoni fault and formation of replacement ore bodies. The Stratoni fault was reactivated in the Neogene by predominately north-south extensional tectonics, which is presently active in the Aegean region (Pavlides and Tranos, 1991; Jolivet et al., 2013).

Ore Deposit Geology

Ore deposits of the Kassandra mining district belong to the NW-trending Serbo-Macedonian metallogenic province within the intrusive belt of the Lece-Chalkidiki metallogenic zone (Fig. 1; Janković, 1997; Serafimovski, 2000) that is dominantly associated with Oligo-Miocene magmatism (Heinrich and Neubauer, 2002). Historic and producing economic deposits include the Trepča skarn district of eastern Kosovo (Strmić-Palinkaš et al., 2013) and the Kiseljak Au-Cu porphyry and polymetallic Au-Ag-Pb-Zn vein system of the Serbian Lece magmatic complex (Dragić et al., 2014). Pipe-like Au-Cu porphyry deposits occur in the southeastern Republic of Macedonia at the Buchim-Damjan-Borov-Dol district and at Llovica (Serafimovski, 2010; Barcikowski et al., 2012; Stefanova et al., 2012). Subeconomic porphyry Cu and skarn prospects also occur in the Vathi area of northern Greece (Kockel et al., 1975; Frei, 1992), to the northwest of the economic Au-Cu porphyry and polymetallic Au-Ag-Pb-Zn-Cu carbonate-replacement deposits within the Kassandra mining district.

Kassandra ore deposits

Olympias: The Olympias deposit was originally described by Neubauer (1957) and Nicolaou (1964), with more recent detailed studies by Kalogeropoulos et al. (1989b) and Kilias et al. (1996). Reevaluation of the deposit-scale geologic framework has been performed by Eldorado Gold Corporation through extensive drilling and relogging campaigns. The carbonate replacement massive sulfide deposit at Olympias is hosted by a sequence of quartzo-feldspathic biotite gneiss interlayered with graphitic marble and amphibolite, bounded to the east by a massive body of megacrystic plagioclase-microcline orthogneiss. Contacts between marble and quartzo-feldspathic biotite gneiss are sharp and conformable. The orebody is localized in a structurally complex zone where marble is deformed by ductile and brittle structures. The regional S_1 fabric of the metamorphic sequence in the deposit area strikes to the northwest and dips steeply northeast, and is locally reworked by isoclinal F_2 folds. A distinct L_2 lineation formed by the intersection of S_1 foliation and S_2 axial planar cleavage is evident within marbles north of the deposit. The metamorphic sequence is disrupted by the NW-trending ductile to semibrittle Kassandra fault and the N-trending East fault (D. Rhys, pers. commun., 2014). Both faults exhibit a similar geometry with apparent normal relative displacement of hanging wall down to the northeast. Marbles that are structurally bound by the Kassandra and East faults host massive sulfide mineralization. A shallow southeast plunge of premineral F_2 folds and L_2 intersection lineation is coincident with the plunge of the Olympias orebody, suggesting that preexisting structures influenced mineralization. The Olympias deposit has a defined downplunge extent of 1,500 m to a depth of approximately 790 m below sea level.

The massive sulfide orebody at Olympias displays a complex sulfide mineral assemblage varying from galena-sphalerite-dominant massive sulfide, to pyrite-rich massive sulfide with traces of arsenopyrite and chalcopyrite. Locally, Zn-Pb-rich sulfide transitions to Au-rich arsenopyrite-bearing massive sulfide, which grades into arsenopyrite- and boulangerite-bearing siliceous breccias. Quartz-rhodochrosite veins containing variable amounts of arsenopyrite and boulangerite occur, particularly in the eastern part of the deposit. Sulfide bodies exhibit coarse- and fine-grained massive and banded textures that cut and replace marble, and are largely discordant to foliation. Locally, however, sulfide banding is concordant with foliation and mimics folded marble layers (Kalogeropoulos et al., 1989b). The latter textures have been interpreted as indicating a predeformation timing, but replacement textures cutting foliation are far more common. Well-preserved rod textures in pyrite, interpreted to be after marcasite, with a sphalerite-rich matrix (Fig. 3A) are common and are observed in other carbonate-replacement deposits (e.g., Leadville, Colorado; Thompson and Arehart, 1990). Sulfide minerals are largely undeformed with some zones showing variable degrees of strain (Kalogeropoulos et al., 1989b). Hahn et al. (2012) constrained the timing of mineralization at Olympias to the Oligo-Miocene based on an arsenopyrite Re-Os age of 26.1 ± 5.3 Ma. This age, along with textural evidence, is consistent with the formation of massive sulfide that postdates major regional Alpine deformation and is likely related to Oligo-Miocene metallogenesis.

Madem Lakkos: The geology of the Madem Lakkos orebody was originally described by Neubauer (1957) and Nicolaou (1964, 1969). The most recent detailed studies were undertaken by Nebel (1989), Nebel et al. (1991), Gilg (1993), Gilg and Frei (1994), and Haines (1998), and the following description of the Madem Lakkos area is largely taken from these studies. The Madem Lakkos carbonate-hosted deposit occurs in a major strand of Stratoni fault within a complexly folded and faulted sequence of amphibolite, marble, and lesser hornblende-bearing quartzo-feldspathic biotite gneiss and fine-grained to aplitic granite gneiss. Contacts between units are commonly sheared within the Stratoni fault zone. The S_1 foliation strikes west-northwest and dips moderately to the southwest in the footwall and north-northwest in the hanging wall. Orebodies are hosted in marble, granite gneiss, and aplite. Mineralization is controlled by faults and hinge zones of shallow E-plunging parasitic F_3 folds. The nearby Stratoni stock is displaced by the WNW-trending Stratoni fault, and is variably affected by fault-controlled hydrothermal alteration and base metal sulfide-bearing veins. The NE-trending right-lateral Vathilakkos fault displaces the Stratoni fault and mineralized massive sulfide bodies at depth (Haines, 1998).

Two stages of sulfide mineralization are recognized at Madem Lakkos. Early replacement-style massive sulfide has

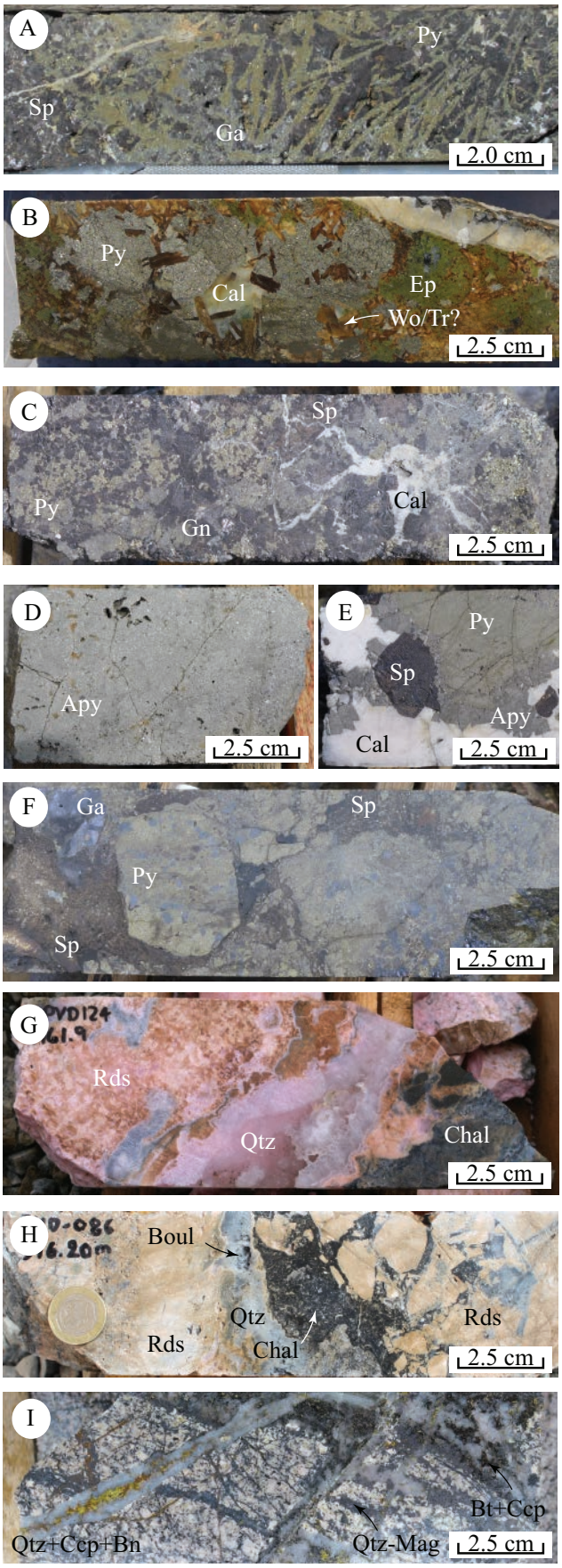

sharp and discordant contacts with host rocks and consists dominantly of galena and sphalerite with lesser pyrite, subordinate chalcopyrite, arsenopyrite, tennantite, tetrahedrite, and rare native gold (Gilg, 1993). Evidence based on deformation textures in sulfide minerals from foliation-parallel and folded sulfide lenses was used to infer a predeformation synsedimentary (syngenetic) origin for mineralization (Nebel et al., 1991). This conclusion has been refuted by Gilg et al. (1992) based on evidence for replacement textures and cross-cutting relationships with respect to tectonic fabric. Moreover, stable and radiogenic isotopes and fluid inclusion data have been used to argue for an epigenetic, postdeformation, replacement origin (Gilg et al., 1992; Gilg, 1993). Nebel et al. (1991) and Gilg (1993) described a second overprinting and volumetrically dominant pyrite-rich disseminated sulfide event that forms the matrix to breccias, and fills or surrounds previous base metal-rich massive sulfide mineralization. The absolute timing of this event is poorly constrained. The sulfide mineral assemblage consists of coarse-grained sphalerite and galena, with lesser chalcopyrite, arsenopyrite, tennantite, tetrahedrite, boulangerite, and a variety of other sulfosalt minerals (Gilg, 1993). Based on K-Ar illite ages, Gilg and Frei (1994) tentatively proposed a late Oligocene age for hydrothermal alteration and mineralization at Madem Lakkos.

East of Madem Lakkos, chalcopyrite-pyrite mineralization is associated with calc-silicate Cu skarn near the contact with the Stratoni stock and associated NE-trending quartz-feldspar porphyry dikes (Gilg, 1993). A prograde mineral assemblage consisting of andradite garnet and diopside with variable anhydrite, epidote, and magnetite is overprinted by a retrograde hydrous mineral assemblage, including iron-rich chlorite after garnet and actinolite ± chlorite after pyroxene and epidote (Gilg, 1993). Chalcopyrite is associated with retrograde alteration accompanied by pyrite, calcite, quartz, epidote, and scheelite (Fig. 3B; Gilg, 1993).

Mavres Petres: The marble-hosted deposit at Mavres Petres occurs 2 km west of Madem Lakkos within the Stratoni fault zone. The orebody occurs over a strike length ~1 km with a SSW-plunging depth extent (defined orebody limit) of about 700 m. The lithologic sequence and S_1 foliation strikes

Fig. 3. Representative mineralization styles from drill core in the Kassandra mining district: (A) massive sulfide from the Olympias deposit displaying bladed pyrite rod textures with sphalerite and galena matrix; (B) skarn mineralization consisting of pyrite with an intergrown calcite and calc-silicate mineral assemblage of epidote-wollastonite-tremolite from the easternmost drilling at the Madem Lakkos deposit; (C) coarse-grained sphalerite-galena-pyrite massive sulfide with minor calcite gangue from the Mavres Petres deposit; (D) fine-grained arsenopyrite-rich massive sulfide from the westernmost drilling of the Mavres Petres orebody; (E) coarse-grained pyrite-arsenopyrite-sphalerite semimassive sulfide with calcite gangue from Mavres Petres; (F) massive sulfide breccia from the Piavitsa prospect consisting of pyritic clasts surrounded and overprinted by galena- and sphalerite-rich sulfide mineralization; (G-H) Au-rich crustiform chalcedony-quartz-rhodochrosite vein and vein breccia containing vug-filling and disseminated needle-form boulangerite from the Piavitsa prospect; (I) typical early quartz-magnetite veins cut by main-stage quartz-magnetite-biotite-chalcopyrite ± bornite veins within the intramineral porphyry at Skouries. Abbreviations: Apy = arsenopyrite, Bt = biotite, Boul = boulangerite, Cal = calcite, Chal = chalcedony, Ccp = chalcopyrite, Ep = epidote, Ga = galena, Mag = magnetite, Py = pyrite, Qtz = quartz, Rds = rhodochrosite, Sp = sphalerite, Tr = tremolite, Wo = wollastonite.

west-northwest subparallel to the Stratoni fault, and becomes NW trending to the north in the footwall of the Stratoni fault. The host lithologies are similar to Madem Lakkos with the exception of a thick granite gneiss body that occurs intercalated with marble in the footwall.

A siliceous Mn oxide gossan forms the surface expression at Mavres Petres and Piavitsa (Gilg, 1993; Arvanitidis and Constantinides, 1994). The orebody at Mavres Petres consists of banded coarse-grained pyrite-sphalerite-galena (Fig. 3C) with minor accessory stibnite and arsenopyrite overprinted by arsenopyrite-bearing siliceous breccias. In the western part of the orebody, the sulfide mineral assemblage becomes pyrite-sphalerite dominant, although locally includes massive arsenopyrite intervals (Fig. 3D-E). Boulangerite occurs as an accessory sulfide mineral interstitial to siliceous breccias, and within quartz-rhodochrosite veins. The partial to complete replacement of fault-bounded marble blocks is evident underground and in drill core from Mavres Petres, documenting the replacement origin of this orebody.

Piavitsa: The Stratoni fault zone loses continuity west of Mavres Petres and appears to jog southward along the contact of granite gneiss with graphite-bearing carbonaceous-biotite schists and marbles (Fig. 2). Drilling at the Piavitsa prospect intersected discontinuous semimassive to massive sulfide lenses, which have undergone synmineral brecciation (Fig. 3F), and prominent siliceous-rhodochrosite ± rhodonite bodies and veins that partially replace and crosscut the host marble (Arvanitidis and Constantinides, 1994). Well-preserved, undeformed Au-bearing rhodochrosite veins display crustiform banded textures (Fig. 3G) with clear crystalline to black chalcedonic silica intergrown with bladed boulangerite, which also occurs as delicate fibrous mat cavity infillings. Mosaic breccia textures with angular fragments of rhodochrosite set in a black chalcedonic silica matrix (Fig. 3H) are interpreted to have formed by hydrothermal brecciation during the later stages of the mineralizing event. Vein and breccia textures are typical of epithermal environments and suggest a relatively shallow, low-temperature setting for Piavitsa compared to carbonate replacement and skarn mineralization to the east.

Skouries: The Skouries Au-Cu porphyry deposit was originally described by Zachos (1963) with subsequent detailed studies by Eliopoulos and Economou-Eliopoulos (1991), Frei (1992, 1995), Tobey et al. (1998), Kroll et al. (2002), and Hahn et al. (2012). The following descriptions are based on work by the authors, which are largely in agreement with observations from previous studies. The Skouries porphyry exhibits four stages of veining and associated alteration. An $^{40}Ar/^{39}Ar$ hydrothermal biotite age of 19.9 ± 0.9 Ma (Hahn et al., 2012) is interpreted as the timing of potassic alteration and mineralization, and is within error of the U-Pb age of the porphyry (20.56 ± 0.48 Ma; Hahn et al., 2012). Stockwork to sheeted quartz-magnetite and magnetite stringer veins and disseminated magnetite alteration locally obliterate the earliest porphyry phase. The majority of the Au-Cu mineralization is interpreted to have been introduced with an intramineral porphyry phase (see "Igneous Petrography" section below) that hosts quartz-magnetite-chalcopyrite veins, and a potassic alteration mineral assemblage consisting of K-feldspar, biotite, and magnetite. A later set of quartz-biotite-chalcopyrite-bornite ± magnetite veins occurs as sheeted to wispy veins and veinlets in the upper parts of the deposit. At depth, these veins become thick (up to 3 cm wide) and sulfide rich, dominated by chalcopyrite ± bornite with envelopes of coarse-grained biotite aggregates (Fig. 3I). This stage of mineralization locally crosscuts or replaces magnetite-bearing veins and disseminated magnetite associated with earlier stages of veining and alteration (D. Rhys, pers. commun., 2014). Platinum and palladium occur as telluride minerals contained in chalcopyrite and as grains within quartz-chalcopyrite ± bornite veins associated with the intramineral porphyry (Eliopoulos et al., 2014; McFall et al., 2016). Gold occurs as inclusions of native metal or electrum in chalcopyrite (Eliopoulos and Economou-Eliopoulos, 1991) or as gold-silver tellurides (McFall et al., 2016).

Postmineral pyrite-carbonate veins with sericite-carbonate-clay alteration overprint earlier mineralization within the stock and adjacent wall rock. An alteration aureole of quartz, calcite, sericite, and pyrite associated with base metal veins has been mapped up to 600 m from the intrusive center, consistent with observations of Tobey et al. (1998). Within 400 m of the porphyry stock, late-distal sericite-pyrite alteration transitions into an early stage, and proximal calc-potassic alteration mineral assemblage consisting of amphibole-biotite-magnetite (Tobey et al., 1998; Kroll et al., 2002). Calc-potassic alteration within the schists is overprinted by K-feldspar associated with main-stage chalcopyrite-bearing veins and disseminated chalcopyrite replacing early magnetite. Supergene enrichment is restricted to a 30- to 40-m-thick zone close to surface consisting of secondary chalcocite and covellite (Tobey et al., 1998).

Igneous Petrology

Previous petrographic studies have been undertaken in the district. The intrusive stock at Stratoni has been previously described by Nikolaou (1960), Tompouloglou (1981), and Kalogeropoulos et al. (1989a, 1990). Frei (1992) further described the Tsikara, Fisoka, and Stratoni stocks and briefly discussed the Aspro Lakkos porphyry intrusion. The Skouries porphyry is described in detail by Frei (1992, 1995), Tobey et al. (1998), and Kroll et al. (2002). The descriptions presented here, while building upon previous studies, are based on field relationships and petrography from 65 thin sections.

Tsikara

The composite monzogabbro-granodiorite intrusion at Tsikara, located south of Stratoni and southeast of Skouries (Fig. 2), is the southernmost and largest postdeformation intrusion within the district, measuring 4.5 km^2 in area. The Tsikara stock intrudes the quartzo-feldspathic biotite gneisses and schists of the Kerdilion unit and occurs within the S-dipping limb of a major F_3 antiform in the footwall of the Gomati fault. Isolated satellite intrusions occur to the north of the main stock and extend south of the Gomati fault within the tectonic mélange of the Athos-Volvi suture zone (Himmerkus et al., 2011). Igneous contacts are sharp, discordant to foliation, and are locally associated with breccias on the western and southwestern margins of the stock. A magnetite-bearing hornfels aureole is variably developed in the metamorphic wall rock. The main stock contains locally abundant subangular xenoliths of gneiss and schist, and less abundant cognate igneous clasts (Fig. 4A).

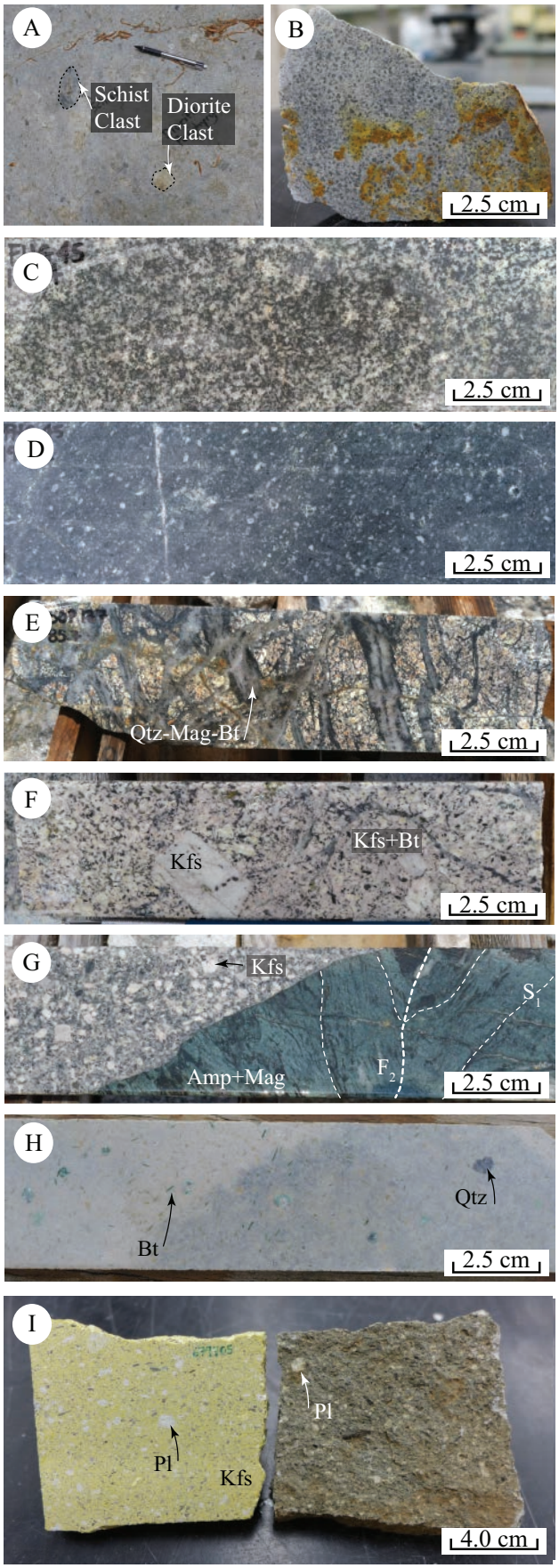

The main stock consists of fine-grained equigranular monzogabbro to monzodiorite and diorite phases, crosscut by a granodioritic microporphyritic phase in the west-central and eastern parts of the Tsikara intrusive complex. The mafic phases have sharp but irregular contacts with the wall rock. The mineralogy of the mafic phases consists of equigranular plagioclase, clinopyroxene, biotite with subordinate microcline, quartz and accessory zircon, apatite, magnetite and ilmenite, and minor pyrite in the groundmass. Chlorite and rare epidote partially replace biotite and clinopyroxene, and plagioclase is selectively replaced by sericite. The crosscutting microporphyry phase (Fig. 4B) contains relict blocky feldspar phenocrysts, which are completely replaced by sericite and set within a fine-grained quartz-sericite-altered groundmass. Unidirectional solidification textures and miarolitic cavities are present within this unit.

Fisoka

The Fisoka stock belongs to a cluster of igneous intrusions that crop out in the hanging wall of the Stratoni fault, northeast of Tsikara and southwest of Stratoni (Fig. 2; Kockel et al., 1975; Tompouloglou, 1981). Each intrusive body is less than 0.2 km^2 in surface area, but the individual pipe-like intrusions may connect at depth. The Fisoka stock is poorly exposed and strongly weathered at surface with limited drilling (seven holes) extending below the weathered zone. The Fisoka intrusions are hosted within variably carbonaceous quartz-biotite gneiss of the Kerdilion unit and interlayered amphibolite. Igneous contacts are largely discordant to metamorphic foliation. Porphyritic phases contain miarolitic cavities similar to those observed in the microporphyritic phase at Tsikara.

Porphyritic stocks and dikes commonly have clast-supported brecciated contacts with wall rock. Breccias are composed of angular gneiss clasts with increasing porphyry clast content adjacent to the coherent porphyry body, and limited matrix consisting of quartz-sericite and pyrite (largely replaced by goethite at surface). Widespread quartz-sericite-pyrite alteration is developed within the metamorphic wall rock, associated with stockwork to sheeted quartz-pyrite veins. Historic drilling for supergene Cu mineralization intersected pervasively bleached porphyry with minor vein and disseminated chalcopyrite and localized secondary chalcocite enrichment at the base of the weathered zone (Kockel et al., 1975).

A swarm of quartz-plagioclase feldspar porphyry dikes exposed between the Fisoka and Stratoni stocks intrude

Fig. 4. Representative surface and drill core examples of Oligo-Miocene intrusive rocks from the Kassandra mining district: (A) monzodiorite at Tsikara with xenoliths of metamorphic wallrock and cognate diorite clast, pencil for scale; (B) microporphyritic granodiorite from Tsikara; (C-D) typical late Oligocene granodiorite and monzodiorite from drill core at Fisoka, respectively; (E) Skouries premineral quartz-monzonite porphyry with characteristic dense network of quartz-magnetite veins; (F) intramineral megacrystic K-feldspar quartz-monzonite porphyry at Skouries displaying strong potassic alteration; (G) late mineral quartz-monzonite porphyry crosscutting folded and amphibole-magnetite-altered gneiss; (H) altered example of the glomerophyric porphyry dike from the Madem Lakkos deposit; (I) black-matrix porphyry dike from the Vathilakkos fault stained with Na-cobaltinitrite to highlight K-feldspar (left) and unstained (right). Abbreviations: Amp = amphibole, Bt = biotite, Kfs = K-feldspar, Mag = magnetite, Pl = plagioclase, Qtz = quartz.

amphibolite in the hanging wall of the Stratoni fault. Contacts are commonly highly brecciated and consist of polymict clast-supported angular blocks of extremely altered metamorphic wall rock (amphibolite with lesser granitic gneiss) and porphyry in an altered matrix. The spatial association of breccias with dikes and extensive alteration suggest a magmatic-hydrothermal or possibly phreatomagmatic origin for the breccias.

The individual Fisoka intrusions are composed of fine- to medium-grained equigranular diorite and granodiorite (Fig. 4C-D) with porphyritic phases to the north. The phenocryst mineralogy consists of K-feldspar, plagioclase, biotite, and clinopyroxene with accessory apatite, titanite, zircon, magnetite, and minor pyrite and subordinate chalcopyrite. Porphyry intrusions are dominated by a crowded interlocking texture consisting of plagioclase ± K-feldspar phenocrysts in a quartz-feldspar-rich groundmass. Chlorite, epidote, titanite, and calcite commonly replace primary biotite and clinopyroxene. Drill core from the Fisoka area reveals an alteration mineral assemblage consisting of sparse to abundant magnetite stringer veinlets associated with aggregates of magnetite and biotite and patchy K-feldspar. The mineralogy and textures are consistent with selective potassic alteration related to a poorly developed porphyry system with minor disseminated chalcopyrite mineralization.

Granodioritic quartz-eye plagioclase feldspar porphyry dikes north of Fisoka are fine grained and consist of plagioclase phenocrysts and rounded quartz phenocrysts displaying resorbed textures. Hydrothermal alteration has resulted in partial replacement of plagioclase phenocrysts and the groundmass by quartz-sericite-pyrite. Clay alteration in surface outcrops may reflect weathering.

Stratoni

The Stratoni stock is a NE-elongated intrusion located north of the village of Stratoni at the eastern end of the Stratoni fault (Fig. 2). The stock has an exposed outcrop area of 1.5 km^2 consisting primarily of granodiorite, with a minor porphyritic phase exposed at the topographically highest part of the stock in the Aspro Chomata prospect area (Gilg and Frei, 1994). The Stratoni stock is hosted by a sequence of quartzo-feldspathic biotite gneisses, amphibolites, and marbles of the Kerdilion unit on the S-dipping limb of a major F_3 antiform within the footwall of the Stratoni fault (Fig. 2). Intrusive contacts are sharp and discordant to metamorphic foliation. Narrow zones of calc-silicate exoskarn locally occur on the western contact of the intrusion within the gneisses. Quartz-sericite-pyrite alteration with pyrite and galena veins occur in the southern half of the stock in proximity to the Stratoni fault. The porphyritic phase of the Stratoni stock exposed at the Aspro Chomata prospect exhibits intense clay-rich alteration related to a dense orthogonal network of quartz-pyrite ± galena veins. Minor secondary malachite staining is present locally on weathered surfaces.

The Stratoni stock is a fine- to medium-grained, equigranular to weakly porphyritic granodiorite with minor diorite phases. Phenocrysts consist of K-feldspar, plagioclase, biotite, and lesser clinopyroxene in a quartz-feldspar groundmass, with accessory apatite, titanite, zircon, magnetite, minor pyrite, and rare chalcopyrite. A pale green color is imparted by chlorite, epidote, titanite, and calcite alteration of primary clinopyroxene and biotite. Feldspars are variably replaced by sericite.

Skouries

The Skouries Au-Cu porphyry, located 8 km south of the Stratoni fault and approximately 1 km to the north of the Gomati fault, is hosted in quartzo-feldspathic biotite gneisses and schists interpreted to be part of the Kerdilion unit. The stock is a pencil-shaped intrusion consisting of multiple quartz monzonite porphyry phases that intrude the S-dipping axis of a regional F_3 antiform (Fig. 2). Outcrop and drill holes define a 200-m-diameter steeply S-plunging intrusive body exceeding 900 m in depth, with porphyry dikes radiating outward from the intrusive center. Intrusive contacts are sharp and discordant to metamorphic foliation and are locally brecciated. Polymict breccias occur in association with syn- to late mineral intrusive phases. These breccias contain altered angular fragments of wall rock and porphyry clasts in a fine-grained dark-gray fragmented matrix, possibly suggesting a magmatic-hydrothermal or phreatic origins.

This study has identified at least four porphyritic intrusive phases at Skouries. The interpreted timing and classification of the intrusive units differ slightly from that proposed by Kroll et al. (2002). The earliest phase, defined by crosscutting relationships, is a dark-gray feldspar porphyry, which hosts an early set of densely sheeted and stockwork quartz-magnetite veins that partially destroy the original igneous textures (Fig. 4E). K-feldspar and plagioclase phenocrysts are set in a fine-grained matrix of K-feldspar, quartz, and primary biotite with accessory titanite and zircon. Phenocrysts and groundmass are extensively overprinted by secondary quartz with abundant disseminated fine-grained magnetite ± biotite.

Au-Cu mineralization is spatially and temporally related to an "intramineral" K-feldspar porphyry corresponding to the pink or main porphyry phase of Kroll et al. (2002). This intrusive phase exhibits a distinct pink coloration imparted by pervasive K-feldspar alteration. The phenocryst mineral assemblage consists of plagioclase and megacrystic K-feldspar with grains reaching up to 3 cm in length (Fig. 4F). Phenocrysts are set in a groundmass dominated by K-feldspar, quartz, amphibole, and accessory titanite and zircon. A finer grained variety of dark-pinkish-gray porphyry crosscuts the earlier intramineral porphyry defined here and may correlate to the intramineral phase of Kroll et al. (2002). This intrusive phase contains K-feldspar and plagioclase phenocrysts with fine-grained disseminated biotite in a K-feldspar-quartz-dominated groundmass, with apatite microphenocrysts, titanite, and zircon occurring as accessory minerals. Both porphyry phases are altered by secondary K-feldspar, quartz, fine-grained biotite, and magnetite with associated disseminated chalcopyrite and bornite.

A final postmineral porphyry phase (Fig. 4G) crosscuts all earlier intrusive phases and associated alteration and mineralized vein sets. The primary mineralogy of this phase is similar to the intramineral porphyry, but veining, potassic alteration, and mineralization are weak to absent. Megacrystic K-feldspar and plagioclase phenocrysts occur in a fine-grained groundmass of K-feldspar, plagioclase, and quartz with accessory titanite, apatite, and magnetite. Pyrite is the dominant sulfide with trace chalcopyrite. Feldspar phenocrysts and

groundmass are commonly clouded, with a pale-green color imparted by weak but pervasive quartz-sericite-carbonate-pyrite alteration.

Aspro Lakkos

A megacrystic K-feldspar porphyry intrusion crops out at Aspro Lakkos approximately 1 km northeast of Skouries. Aspro Lakkos is a sill-like body that intrudes the northeast limb of a major F_3 antiform subparallel to foliation (Fig. 2). Discordant contacts are generally brecciated containing a polymictic suite of angular to subangular clasts of sericite-altered schist and porphyry fragments in a fine-grained sericite-altered igneous matrix, suggesting a possible magmatic-hydrothermal origin. Rare and discrete clast-supported breccia dikes crosscut the Aspro Lakkos body. These breccias are composed of angular to rounded wall-rock fragments and porphyry clasts, some of which exhibit irregular shapes, contained in a fine-grained milled schistose matrix, suggesting phreatic brecciation. A weak pervasive sericite overprint with localized zones of strong quartz-sericite-pyrite alteration are common. Porphyry dikes of similar texture and composition are observed splaying from the main body in a northwest-southeast direction along foliation. A late set of fine-grained black-matrix porphyry dikes crosscut the main megacrystic porphyry body in a northwest orientation, also parallel to the regional structural fabric.

The main Aspro Lakkos porphyry is texturally similar to the late porphyry phase at Skouries, with prismatic plagioclase and megacrystic K-feldspar phenocrysts (upward of 3 cm in length) occurring with fine-grained euhedral biotite books, quartz, and lesser apatite microphenocrysts. K-feldspar and quartz comprise the groundmass with accessory zircon, magnetite, and subordinate pyrite. Quartz phenocrysts are generally subrounded, and occasionally display irregular embayment textures. Some quartz and carbonate grains display undulose textures, suggesting a possible metamorphic xenocrystic origin. Secondary carbonate, sericite, and pyrite variably replace feldspars, biotite, and groundmass.

Black-matrix porphyry dikes

Porphyritic dikes displaying prominent trachytic (or microlitic) texture were originally described as andesitic dacites by Neubauer (1957) and reclassified as lamprophyres by Nicolaou (1960) and Kalogeropoulos et al. (1991). Nebel et al. (1991) described andesite and rhyodacite dikes with resorbed quartz phenocrysts at Madem Lakkos. This study documents two sets of porphyritic dikes defined by the presence or absence of a distinct glomero porphyritic (glomerophyric) texture.

Glomerophyric dikes: Glomerophyric dikes crop out within the Stratoni fault corridor, intercepted in drill core at Piavitsa, and are present underground at Madem Lakkos (Nebel et al., 1991; Haines, 1998) and Olympias (Kalogeropoulos et al., 1989b). They typically range from 1 to 2 m in width, trend north-northeast, and have sharp contacts that are discordant to metamorphic foliation. Contacts are commonly unbrecciated. Dikes display variable degrees of quartz-sericite-carbonate-pyrite alteration or can be unaltered. These dikes contain aggregates of quartz and less commonly K-feldspar phenocrysts (Fig. 4H). Abundant needle-shape phlogopitic biotite defines a flow-banded texture. Accessory euhedral apatite microphenocrysts are common. Unaltered groundmass is typically dark gray, consisting of fine-grained quartz and K-feldspar. Quartz phenocrysts are typically rounded, commonly showing corroded, resorbed rims or embayment textures enveloped by fine-grained secondary sericite-carbonate-clay alteration. Chlorite replaces biotite, and sericite-carbonate partially replace the groundmass and feldspar phenocrysts. Most dikes contain disseminated magnetite and trace pyrite, and pyrite content increases systematically with the intensity of quartz-sericite-carbonate alteration. While these biotite-quartz-feldspar porphyry dikes have been previously classified as calc-alkaline lamprophyre minettes by Kalogeropoulos et al. (1991), their felsic phenocryst mineralogy precludes the lamprophyre classification (e.g., Rock, 1991).

Nonglomerophyric dikes: Black-matrix porphyry dikes in the Aspro Lakkos area contain fine-grained K-feldspar and plagioclase phenocrysts, euhedral biotite books, and accessory apatite microphenocrysts in a dark, near-aphanitic K-feldspar-rich groundmass. Inclusions of rounded to irregularly shaped fragments of highly strained quartz and carbonate are common, probably representing deformed metamorphic wall-rock fragments. Disseminated magnetite occurs in the groundmass along with fine-grained pyrite associated with weak pervasive sericite-carbonate alteration. A black-matrix porphyry dike intrudes the Vathilakkos fault (Fig. 4I) near Madem Lakkos (Fig. 2). A prominent flow texture is defined by the alignment of evenly distributed and abundant hornblende and biotite phenocrysts with lesser K-feldspar, plagioclase, quartz, and sparse clinopyroxene in a fine-grained dark-gray K-feldspar-rich groundmass. Rare and widely dispersed K-feldspar megacrysts are evident. Accessory minerals include apatite microphenocrysts, zircon, and titanite. Disseminated magnetite and rare chalcopyrite occur in the groundmass. Minor sericite-carbonate-clay alteration preferentially replaces clinopyroxene and the rims of plagioclase and K-feldspar phenocrysts.

Zircon U-Pb Geochronology

Previously published geochronology within the district was based on the K-Ar dating (Papadakis, 1971; Burgarth et al., 1980; Tompouloglou, 1981) with limited zircon U-Pb data collected from the Tsikara composite stock, Stratoni stock, and Skouries porphyry (Frei, 1992; Gilg and Frei, 1994; Hahn et al., 2012). Here we present 13 new zircon U-Pb ages of igneous intrusions from the Kassandra mining district. The data are consistent with major magmatic events in the late Oligocene and early Miocene as suggested by previous authors (Fig. 5).

Methods

Samples were collected in the field from least altered and weakly weathered surface outcrops. Analyses were conducted at the Pacific Center for Isotopic and Geochemical Research (PCIGR) at the University of British Columbia in Vancouver, Canada. Sample preparation and U-Pb analytical methods are adapted from Tafti et al. (2009). Samples were pulverized using a conventional crushing and grinding circuit. Zircon separation was performed using a Wilfley gravity separation table, heavy liquid, and Frantz magnetic-separator techniques.

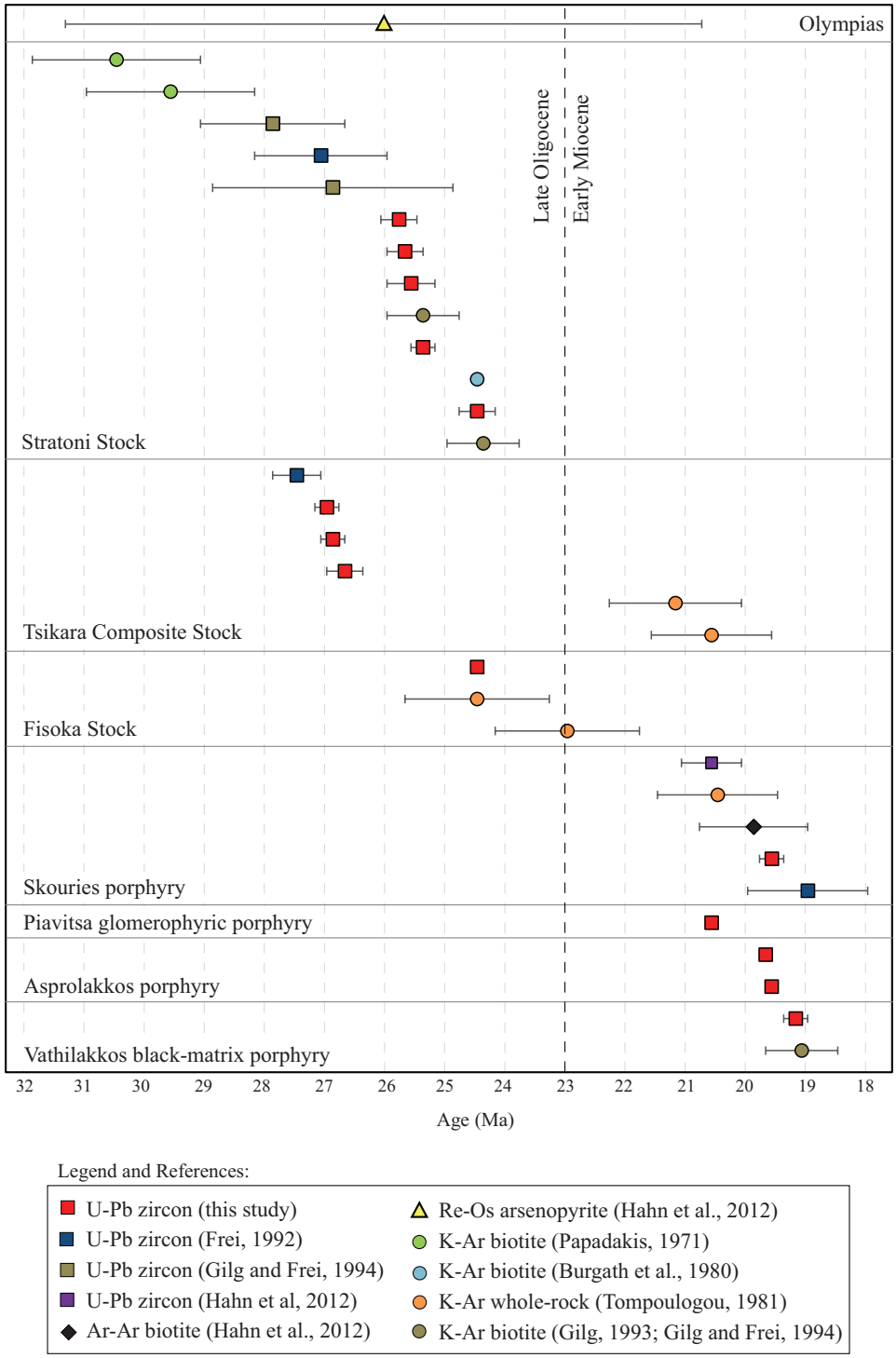

Fig. 5. Geochronology compilation of Oligo-Miocene intrusive rocks from the Kassandra mining district sourced from previously published work and this study. Uncertainties for U-Pb, $^{40}Ar/^{39}Ar$, Re-Os, and K-Ar dates are reported at the 2σ level.

Zircons greater than about 50 μm in diameter were handpicked from the mineral separates and were mounted in a thermal-setting epoxy puck beside several grains of the 337.13 ± 0.13 Ma Plešovice zircon standard (Sláma et al., 2008) and the 416.78 ± 0.33 Ma Temora-2 reference zircon (Black et al., 2004). The zircon-embedded epoxy puck was brought to a high polish and the surface washed for 10 min with dilute nitric acid and rinsed in ultraclean water prior to analysis. Portions of the grains of the highest quality (e.g., little evidence for alteration, inclusions, or possible inherited cores) were selected for analysis. Each grain was imaged using cathodoluminescence to help guide analysis.

A laser ablation inductively coupled plasma mass spectrometer (LA-ICP-MS) was employed for U-Pb zircon analysis. Samples were mounted into a New Wave UP-213 laser ablation cell coupled with a Thermo Finnigan Element2 single collector, double-focusing, magnetic sector ICP-MS. A laser spot diameter of 30 μm was used at 42% power. Line scans rather than spot analyses were employed to minimize elemental fractionation during the analyses. Background data were measured with the laser shutter closed for 10 s, followed by data collection with the laser firing for approximately 35 s. The time-integrated signals were analyzed using Iolite software (Paton et al., 2011), which automatically subtracts background measurements, propagates all analytical errors, and calculates isotopic ratios and dates. Corrections for mass and elemental fractionation were made by bracketing analyses of unknown grains with replicate analyses of the Plešovice zircon standard. Final interpretation and plotting of the analytical results employed the ISOPLOT v. 3.09 geochronological software of Ludwig (2003).

Tsikara composite stock

Three different intrusive phases compose the Tsikara composite stock and are interpreted, on the basis of geologic mapping and geochemistry, to be part of the same intrusive event. Three samples were collected from each phase to test this hypothesis.

Sample 593870: Eighteen zircon grains were analyzed from an unaltered dark clinopyroxene-bearing diorite from the northern half of the composite stock. All analyses fall on or near Concordia with one grain giving a slightly younger age interpreted to be the result of postcrystallization Pb loss (Fig. 6A). The remaining 17 analyses yielded a calculated weighted average $^{206}Pb/^{238}U$ age of 27.00 ± 0.19 Ma (Fig. 6B; mean squared of weighed deviates [MSWD] = 1.4; probability of fit = 0.14). We interpret this age to reflect the crystallization age of the main phase in the Tsikara stock.

Sample 593871: Twenty zircons were analyzed from a sericite-altered and weakly porphyritic granodiorite that intrudes the clinopyroxene-bearing diorite. Four grains gave significantly older $^{206}Pb/^{238}U$ ages and are interpreted to be basement-derived xenocrysts. A 602 Ma age marks the oldest zircon recognized in this survey and may be derived from Neoproterozoic basement. Two xenocryst grains yielding $^{206}Pb/^{238}U$ ages of 340 and 250 Ma are consistent with the age of the underlying Permo-Carboniferous Kerdilion unit and Triassic rift-related granites (e.g., Arnea granite), respectively. One zircon grain gave a $^{206}Pb/^{238}U$ age of 39.5 Ma, interpreted as a xenocryst possibly corresponding to the regional pegmatite event within the Kerdilion unit (Kalogeropoulos et al., 1989b). The remaining 16 zircon grains cluster on Concordia with a weighted average $^{206}Pb/^{238}U$ age of 26.65 ± 0.31 Ma (Fig. 6C-D; MSWD = 1.3; probability of fit = 0.20). This date is interpreted as the crystallization age of a younger fractionated phase of the Tsikara stock.

Sample 593882: Seventeen zircons were analyzed from an unaltered salt-and-pepper-textured diorite phase intruding the clinopyroxene-bearing stock. All analyses plot on or near Concordia yielding a weighted average $^{206}Pb/^{238}U$ age of 26.92 ± 0.20 Ma (Fig. 6E-F; MSWD = 1.7; probability of fit = 0.047). This date corroborates the other ages and is interpreted as the crystallization age of an intermediate composition phase within the composite stock.

Fisoka stock

The Fisoka intrusive cluster is largely granodiorite in composition with porphyritic phases evident to the northeast near Stratoni. On the basis of petrology (see "Petrochemistry" section below), the Fisoka stock is similar to the Tsikara composite stock to the southwest and the Stratoni stock to the northeast. One surface sample was collected from a porphyritic body in the Fisoka area to test this hypothesis.

Sample 279446: Twenty zircons were analyzed from a sericite-altered crowded feldspar porphyry intrusion, coincident with an area of minor supergene Cu mineralization (Kockel et al., 1975). All zircon grains analyzed cluster on or near Concordia resulting in a weighted average $^{206}Pb/^{238}U$ age of 24.47 ± 0.14 Ma (Fig. 6G-H; MSWD = 0.82; probability of fit = 0.69). This age is interpreted as the crystallization age of the porphyry phase of the Fisoka intrusive cluster.

Stratoni stock

Gilg and Frei (1994) published zircon U-Pb ages of 27.1 ± 1.1 and 26.9 ± 2.0 Ma for the Stratoni stock, and 27.9 ± 1.2 Ma for the porphyritic phase at Aspro Chomata (Fig. 5). Low precision and large errors are attributed to a low $^{206}Pb/^{204}Pb$ ratio that necessitated a common lead correction at 30 Ma (Frei, 1992). Thus, reevaluation of these dates using modern techniques was warranted. This study analyzed two representative samples collected from the equigranular plutonic stock, and the internal porphyritic phase from the Aspro Chomata prospect area, respectively.

Sample 679714: Twenty zircon grains were analyzed from a weakly porphyritic phase of quartz-feldspar granodiorite exposed at Aspro Chomata (Fig. 2). The prospect is associated with minor disseminated copper mineralization and poorly developed porphyry-style veins, overprinted by sheeted base metal sulfide-bearing quartz veins and associated intense bleaching and clay alteration. All analyses fall on Concordia; however, the data show considerable scatter ranging from 23.83 to 26.63 Ma (Fig. 7A). A subset of the 11 youngest grains yielded a weighted average $^{206}Pb/^{238}U$ age of 24.53 ± 0.31 Ma (Fig. 7A-B; MSWD = 2.0; probability of fit = 0.03). A subset of the 12 oldest grains resulted in a weighted average $^{206}Pb/^{238}U$ age of 25.78 ± 0.31 Ma (Fig. 7A-B; MSWD = 1.9; probability of fit = 0.04). We interpret these data to represent two stages of magmatism: the older zircons are likely antecrysts recording crystallization of the progenitor granodiorite, whereas the slightly younger zircons may reflect crystallization of the more differentiated porphyritic phase.

Sample 593580: Twenty zircon analyses were performed on the topographically lowest exposed portion of nonporphyritic equigranular quartz-feldspar granodiorite. Nearly all the zircon grains fall on Concordia with minor scatter, yielding a weighted average $^{206}Pb/^{238}U$ age of 25.36 ± 0.15 Ma (Fig. 7C-D; MSWD = 1.4; probability of fit = 0.10). This age is interpreted as the crystallization age of the Stratoni granodiorite and is the same age within error as the interpreted older age from Aspro Chomata. The age of the Stratoni granodiorite also places an upper age limit on synmineral, semibrittle

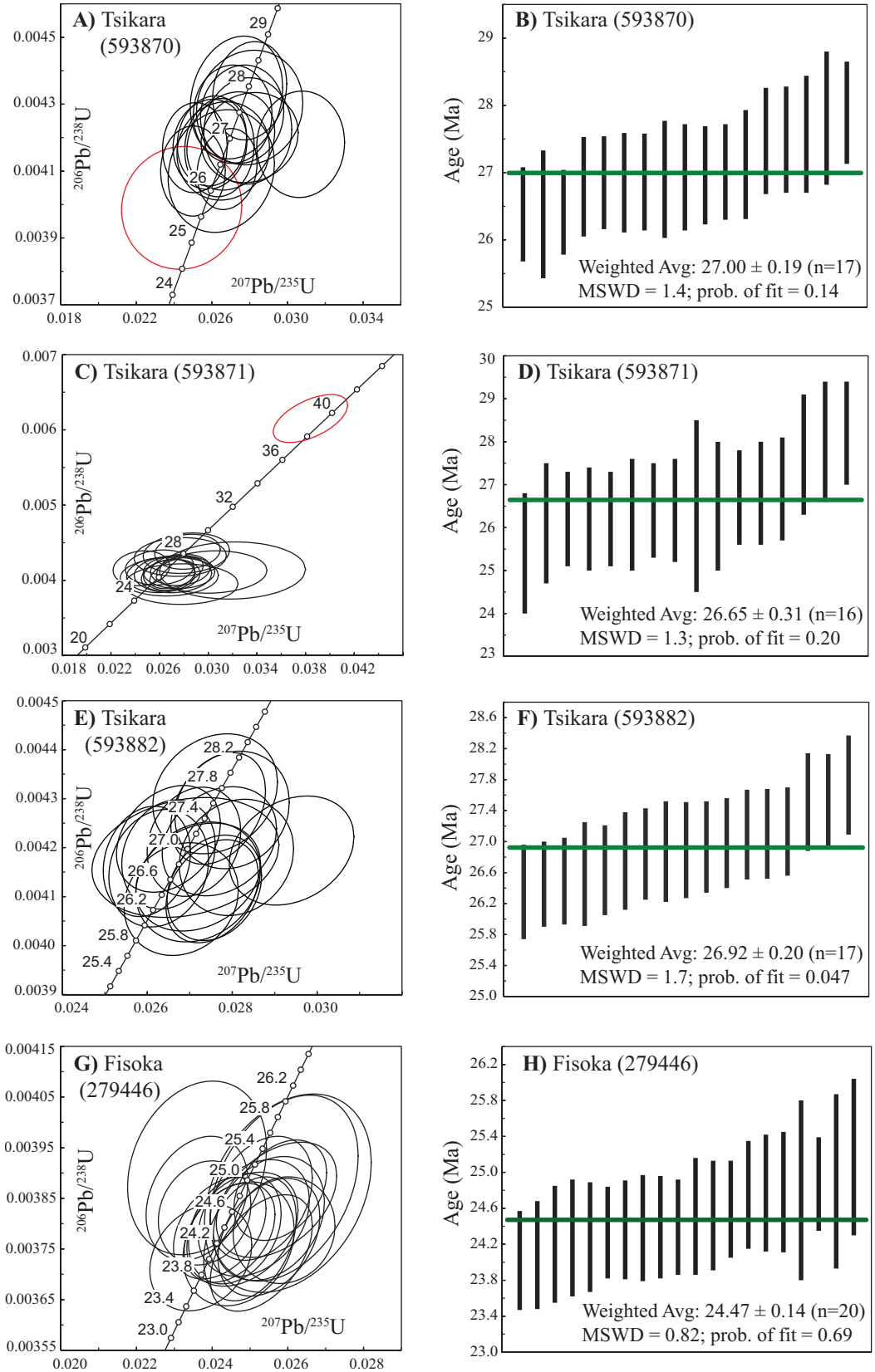

Fig. 6. Zircon U-Pb Concordia and weighted average $^{206}Pb/^{238}U$ age plots of late Oligocene intrusive rocks from the composite Tsikara stock (A-F) and the Fisoka stock (G-H). Data point errors are reported at the 2σ level. Red ellipses correspond to rejected analyses.

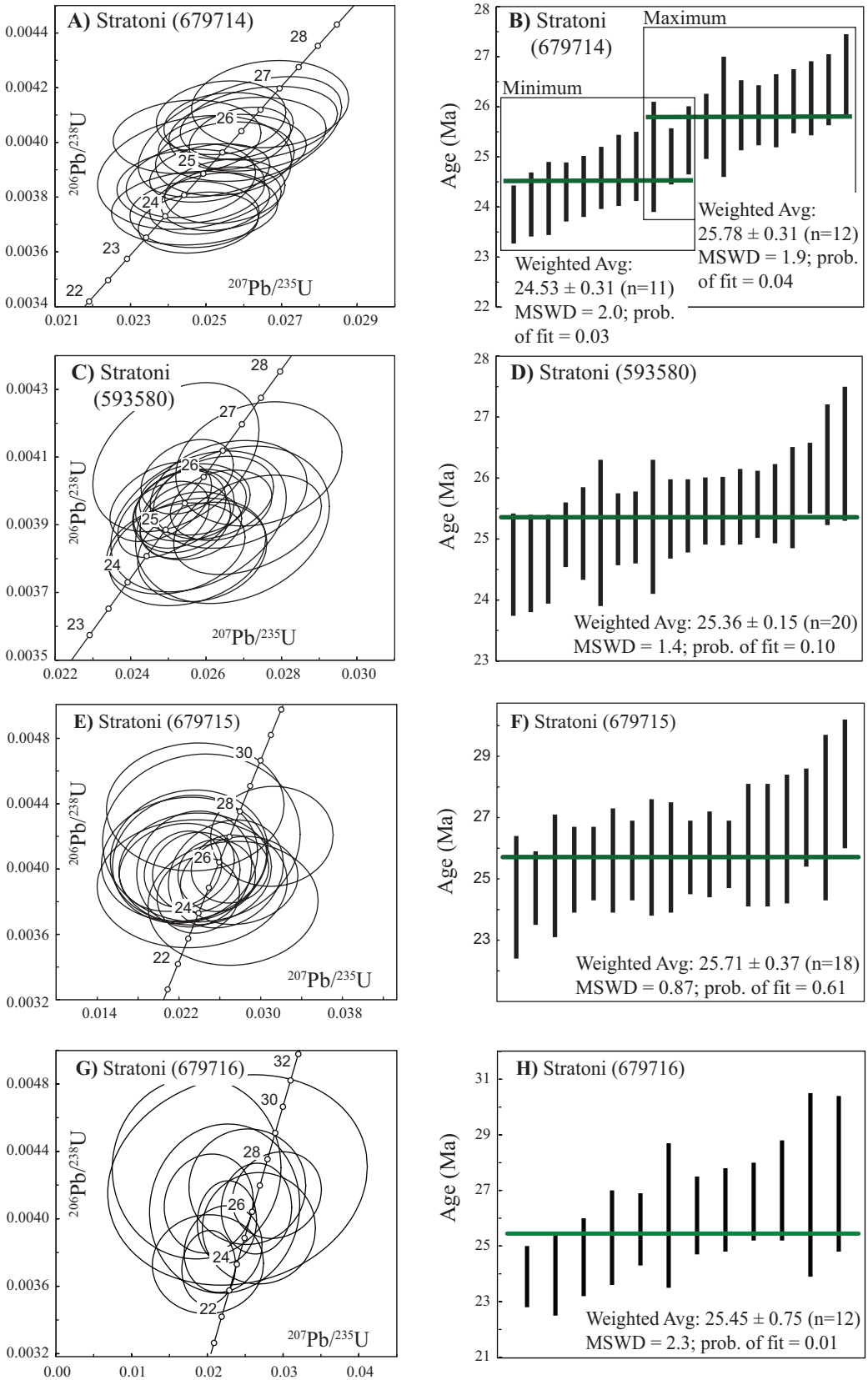

Fig. 7. Zircon U-Pb Concordia and weighted average $^{206}Pb/^{238}U$ age plots of late Oligocene intrusive rocks from the Stratoni stock (A-D) and quartz-feldspar porphyry dikes (E-H) at Stratoni. Data point errors are reported at the 2σ level.

deformation and associated hydrothermal alteration related to the Stratoni fault.

Stratoni quartz-feldspar porphyry dikes

Granodioritic quartz-feldspar porphyry dikes in the Stratoni area are similar in texture and geochemistry to the porphyry intrusions at Fisoka. Two samples were collected east of the Madem Lakkos orebody near the contact with the Stratoni stock: one from a brecciated porphyritic body, and a second from a quartz-feldspar porphyry dike that crosscuts the breccia.

Sample 679715: Twenty zircons were analyzed from the brecciated and quartz-sericite-pyrite-altered quartz-eye feldspar porphyry. One grain resulted a $^{206}Pb/^{238}U$ age of 153.7 Ma interpreted as a xenocryst likely derived from a Late Jurassic to Early Cretaceous intrusive event that affected the Rhodope basement (Turpaud and Reischmann, 2003; Himmerkus et al., 2011). A second grain yielded a $^{206}Pb/^{238}U$ age of 32.7 Ma which lies outside the expected error and was rejected. The remaining 18 grains plot very near Concordia and have a weighted average $^{206}Pb/^{238}U$ age of 25.71 ± 0.37 Ma (Fig. 7E-F; MSWD = 0.87; probability of fit = 0.61). This age is interpreted to be the crystallization age of the dike.

Sample 679716: Twenty zircons were analyzed from an altered quartz-eye feldspar porphyry dike cutting the brecciated porphyry previously described. Two older populations of zircons were identified with four grains yielding a range of $^{206}Pb/^{238}U$ ages from 171.0 to 150.8 Ma. These zircons appear to be xenocrystic possibly representing basement of uncertain affinity. Four younger grains resulted in a range of $^{206}Pb/^{238}U$ ages from 49.3 to 41.8 Ma and are interpreted as xenocrysts corresponding to the Late Cretaceous to early Eocene intrusive event (De Wet et al., 1989; Frei, 1996; Bébien et al., 2001). The remaining 12 grains plot on or near Concordia with minor scatter (Fig. 7G) possibly due to minor Pb loss as indicated by the elevated MSWD (2.3) and low probability of fit (0.01), and a relatively imprecise weighted average $^{206}Pb/^{238}U$ age of 25.45 ± 0.75 Ma (Fig. 7H). This date is within error of the older brecciated porphyry, suggesting multiple intrusive episodes and brecciation associated with this magmatic event.

Skouries

A previously published LA-ICP-MS single grain zircon U-Pb age of 20.56 ± 0.48 Ma from the Skouries stock (Hahn et al., 2012) probably represents the crystallization age of the synmineral porphyry phase. One sample was collected from a distal porphyry dike and, on the basis of petrology, appears to be similar to the late- to postmineral porphyry intrusive phases at Skouries. This sample is intended to test the timing relationship of the dike with the published crystallization age at Skouries.

Sample 593567: Twenty zircons were analyzed from a quartz-sericite-pyrite-altered megacrystic K-feldspar porphyry dike located 0.5 km south of the mineralized stock. One grain gave an older $^{206}Pb/^{238}U$ age of 44.7 Ma and is interpreted to be a xenocryst associated with the Late Cretaceous to early Eocene intrusive event (De Wet et al., 1989; Frei, 1996; Bébien et al., 2001). Two grains give older results that lie outside the expected error and were rejected. The remaining 17 zircon grains plot on or near Concordia (Fig. 8A), but with significant scatter as indicated by the high MSWD (3.5) and low probability of fit (0.0). The weighted average $^{206}Pb/^{238}U$ age is 19.59 ± 0.17 Ma (Fig. 8B), but given the scatter in the data the interpreted crystallization age for the porphyry dike is tentative. Nevertheless, the age is likely coeval with other similar dikes emanating from the Skouries stock and the postmineral megacrystic K-feldspar porphyry observed within drill core at Skouries.

Aspro Lakkos

Geologic mapping identified black-matrix porphyry dikes that crosscut the megacrystic K-feldspar porphyry of Aspro Lakkos. One sample was analyzed from the megacrystic porphyry and one from a crosscutting dike to constrain their absolute age of emplacement and to compare these results to compositionally similar phases at Skouries and Vathilakkos. No published U-Pb data exist from Aspro Lakkos.

Sample 593587: Twenty zircon grains were analyzed from the weakly sericite-pyrite-altered megacrystic K-feldspar porphyry at Aspro Lakkos. All 20 grains resulted in overlapping concordant analyses yielding a weighted average $^{206}Pb/^{238}U$ age of 19.71 ± 0.10 Ma (Fig. 8C-D; MSWD = 1.6; probability of fit = 0.059). This age is interpreted as the crystallization age of the Aspro Lakkos porphyry intrusion, approximately coeval with the emplacement of the late porphyry phase at Skouries.

Sample 593586: Twenty zircon grains were analyzed from a barren black-matrix K-feldspar porphyry dike crosscutting the main Aspro Lakkos porphyry body. Three grains were rejected on the basis of large analytical errors and skewness. The remaining 17 grains plot on or near Concordia with minor scatter (Fig. 8E). The weighted average yielded a $^{206}Pb/^{238}U$ age of 19.58 ± 0.14 Ma (Fig. 8F; MSWD = 1.9; probability of fit = 0.016) and is interpreted to be the crystallization age of this late-stage dike which is effectively coeval with the porphyry. The age of the dike may represent the age of other texturally similar dikes in the district.

Piavitsa

A series of NNE-trending glomerophyric porphyry dikes crop out within the Stratoni fault zone in the Piavitsa area approximately 5 km north of Aspro Lakkos (Fig. 2). A surface sample was collected from an unmineralized dike that crosscuts the siliceous-rhodochrosite ± rhodonite body hosted within the Stratoni fault. No known U-Pb data exist for these dikes.

Sample 279433: Twenty zircon grains were analyzed from a sericite-pyrite-altered glomerophyric quartz porphyry dike. Six grains returned two older populations: 51.60 to 42.32 Ma, and 26.99 to 24.15 Ma. These zircons are interpreted as xenocrysts consistent with ages from the Late Cretaceous to early Eocene (De Wet et al., 1989; Frei, 1996; Bébien et al., 2001) and late Oligocene intrusive events, respectively. The 14 remaining analyses plot on or near Concordia with a weighted average $^{206}Pb/^{238}U$ age of 20.62 ± 0.13 Ma (Fig. 8G-H; MSWD = 0.95; probability of fit = 0.50), interpreted as the crystallization age of the dike. This age suggests that glomerophyric porphyry dikes that occur in the area are similar in age to the Skouries porphyry (within 1 m.y.). The crosscutting relationship of this early Miocene dike with the siliceous-rhodochrosite

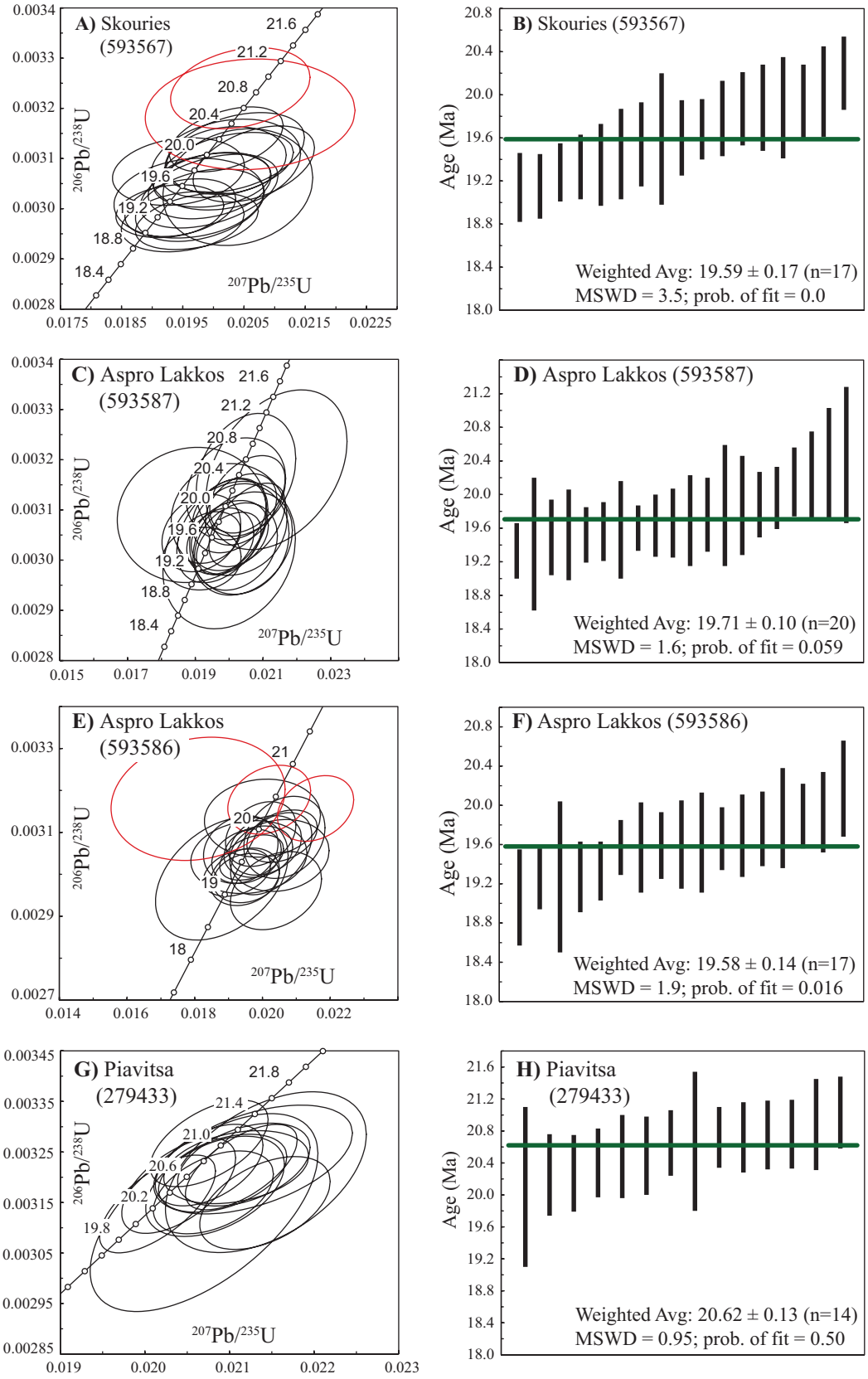

Fig. 8. Zircon U-Pb Concordia and weighted average $^{206}Pb/^{238}U$ age plots of early Miocene intrusive rocks at Skouries (A-B), Aspro Lakkos (C-F), and the glomerophyric porphyry dike at the Piavitsa prospect (G-H). Data point errors are reported at the 2σ level. Red ellipses correspond to rejected analyses.

± rhodonite carbonate replacement body provides a younger age limit for mineralization at Piavitsa.

Vathilakkos

A black-matrix porphyry dike occurs within the Vathilakkos fault (Fig. 2), both of which crosscut the massive sulfide orebody at the Madem Lakkos deposit. This dike has been dated previously at 19.1 ± 0.6 by the K-Ar method (Gilg and Frei, 1994).

Sample 679705: Seventeen zircon grains were analyzed from the unaltered K-feldspar-hornblende-biotite porphyry dike. Ten zircon grains returned significantly older ages with a population of eight grains that range from 183.3 to 250.8 Ma. These zircons are interpreted as xenocrysts possibly reflecting Triassic to Jurassic age basement. One zircon grain plots at 51.3 Ma (Fig. 9A) and is interpreted to be a xenocryst consistent with the age of the Ierissos granite (Frei, 1996). One zircon grain lies skewed from the main age cluster at 22.4 Ma and was rejected on this basis. Seven of the remaining zircon grains plot on or near Concordia with a weighted average $^{206}Pb/^{238}U$ age of 19.21 ± 0.19 Ma (Fig. 9A-B; MSWD = 1.2; probability of fit = 0.28), interpreted as the crystallization age of the Vathilakkos porphyry dike. This provides a younger age limit on mineralization at Madem Lakkos as previously recognized by Gilg and Frei (1994).

Summary

Two intrusive suites have been defined by the new geochronological results, supporting previous geochronology in the region (Frei, 1992). The composite stock at Tsikara and the Fisoka and Stratoni stocks define a late Oligocene igneous suite emplaced in the Kerdilion unit from 27 to 24.5 Ma. The porphyry stocks and dikes at Skouries and Aspro Lakkos, as well as the porphyritic dikes at Piavitsa and Vathilakkos define an early Miocene igneous suite restricted to a period from 20.5 and 19.2 Ma.

Petrochemistry

Methods

Eighty-five representative samples of Oligo-Miocene intrusive rocks were collected from surface and drill core for whole-rock geochemistry. Least altered samples were collected where possible; however, some show incipient alteration and weathering that may influence major element chemistry. Whole-rock geochemical analyses were completed at Acme Labs in Vancouver, British Columbia. Major and minor element analyses were determined by inductively coupled plasma mass spectroscopy (ICP-MS) and inductively coupled plasma optical emission spectroscopy (ICP-OES) after lithium metaborate and tetraborate fusion. Carbon and sulfur were determined by Leco methods and ferrous iron was measured by titration. Analytical accuracy and precision determined from internationally certified reference standards and duplicates, respectively, are within 5 relative percent for major oxides and within 10 relative percent for most minor and trace elements (calculation methods after Piercey, 2014).

Major and trace element geochemistry

Late Oligocene magmatism: Data plotted on the total alkali versus silica diagram (Fig. 10A) show a broad distribution of compositions ranging from monzogabbro to monzonite for the main stock at Tsikara, with subordinate monzodiorite to gabbrodiorite phases in the central stock at Fisoka. More evolved compositions range from diorite to granodiorite in the Stratoni and Fisoka stocks, including a granodiorite microporphyry phase crosscutting the mafic stock at Tsikara. The data show a negative sloping trend in the granodiorite field interpreted to reflect incipient alteration and weathering of surface samples predominately from the Tsikara microporphyry and porphyry dikes at Fisoka. The suite is subalkaline as defined by the classification of Irvine and Baragar (1971) and falls in the high K calc-alkaline magma series (Fig. 10C). Petrographic evidence suggests that sericitic alteration in some samples correlates with elevated K_2O concentrations in the granodiorite porphyry at Tsikara as well as porphyry dikes north of Fisoka, resulting in apparent shoshonitic compositions (Fig. 10C).

The late Oligocene igneous rocks are relatively enriched in light rare earth elements (LREE) whereas heavy rare earth elements (HREE) show flat signatures when normalized to chondritic values (Fig. 11A-C). The Sm/Yb ratio is utilized to model HREE fractionation (e.g., Kay and Mpodozis, 2001; Bissig and Tosdal, 2009). Sm/Yb ratios from the mafic stock

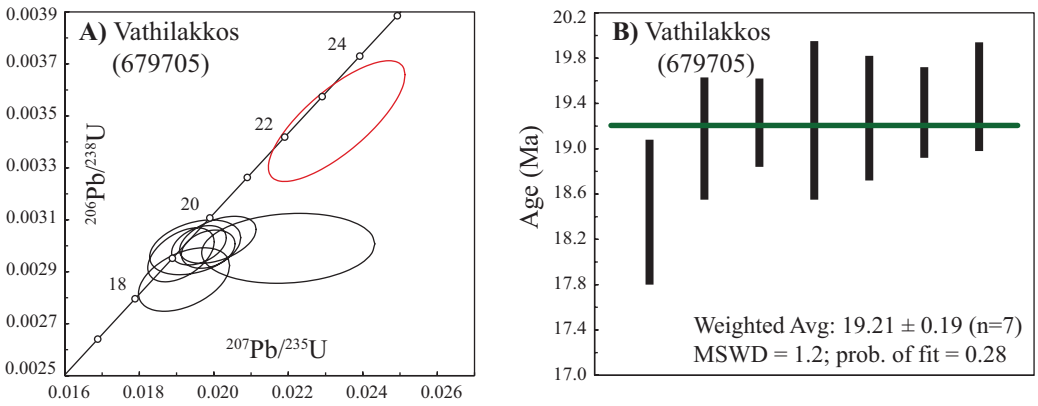

Fig. 9. Zircon U-Pb Concordia and weighted average $^{206}Pb/^{238}U$ age plots for the early Miocene black-matrix porphyry dike at Vathilakkos (A-B). Data point errors are reported at the 2σ level. Red ellipses correspond to rejected analyses.

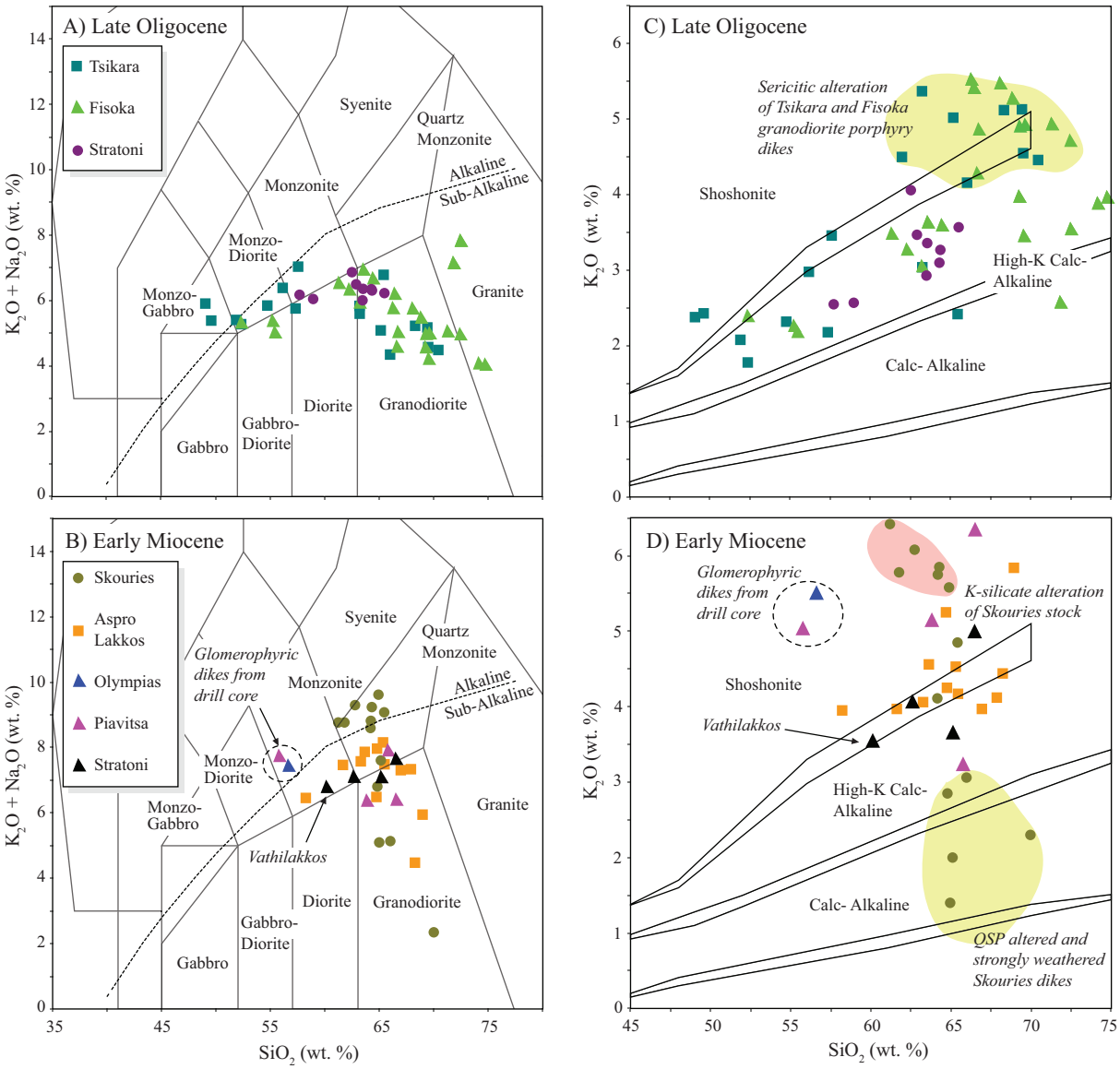

Fig. 10. Geochemical classification of late Oligocene and early Miocene igneous rocks of the Kassandra mining district: (A-B) Total-alkali vs. silica diagram for plutonic igneous rocks of Middlemost (1994) with alkaline-subalkaline division represented by dotted line after Irvine and Baragar (1971). Early Miocene porphyry dikes represented by (pink, blue, and black) triangles are referred to by their volcanic equivalents in the text; (C-D) K_2O vs. SiO_2 subalkalic discrimination diagram after Rickwood (1989). Fields shaded in yellow and red correspond to samples that have experienced strong quartz-sericite-pyrite (QSP) alteration or K-silicate alteration, respectively.

and microporphyry at Tsikara (1.23–3.33) as well as the stocks at Fisoka (1.38–2.66) and Stratoni (1.78–2.36) suggest minimal to no HREE fractionation (Fig. 12A). The porphyry dikes north of Fisoka show minor HREE fractionation patterns (Sm/Yb = 1.74–4.72) with the most fractionated values from aplitic granite dikes. La/Yb ratios are generally <20 for all stocks and slightly elevated (17.46–51.83) for porphyry dikes north of Fisoka (Fig. 12C). Sr/Y ratios for the late Oligocene intrusive suite range from 0.33 to 69.59, where the most depleted values reflect alteration. The average Sr/Y ratio (37.22) from unaltered Stratoni stock samples is likely representative of the Sr/Y ratio for the late Oligocene suite. A wide range of Eu_n/Eu^* values (0.55–0.96; Fig. 12A) suggests that the REE pattern was controlled primarily by feldspar fractionation rather than amphibole (Hanson, 1980).

Incompatible large ion lithophile elements (LILE) have high concentrations in the late Oligocene suite. Strontium concentrations are extremely high with respect to average upper crustal abundance (320 ppm Sr; Rudnick and Gao, 2003) reaching values as high as 912 ppm at Stratoni, 897 ppm at Tsikara, and 827 ppm at Fisoka. Barium is similarly enriched with respect to average upper continental crust (624 ppm Ba; Rudnick and Gao, 2003) with concentrations of up to 1,136 ppm at Tsikara, 1,025 ppm at Stratoni, and 935 ppm at Fisoka. Uranium and Th concentrations are anomalous with respect to average upper continental crust

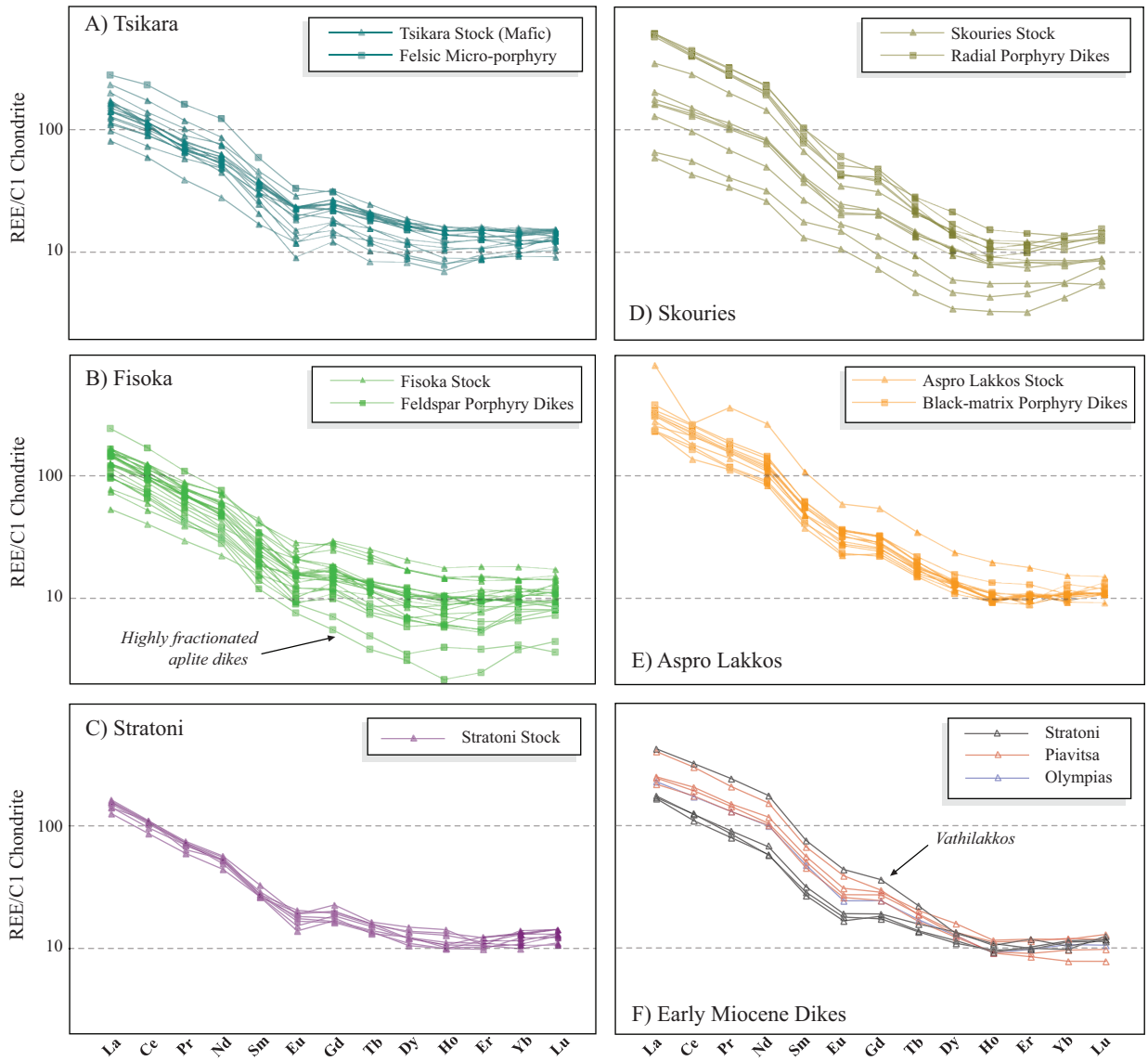

Fig. 11. Chondrite-normalized REE patterns for (A-C) late Oligocene and (D-F) early Miocene igneous rocks. Normalization values are those of Sun and McDonough (1989).

(2.6 ppm U, 10.0 ppm Th; Rudnick and Gao, 2003). The highest U and Th values for the suite occur at Tsikara with concentrations up to 14 and 33 ppm, respectively. The elevated LILE and peraluminous character (alumina saturation index >1) of these intrusive rocks suggest high degrees of crustal contamination.

Early Miocene magmatism: Skouries and the barren Aspro Lakkos porphyries are quartz monzonites based on their total alkali versus silica contents (Fig. 10B). Kroll et al. (2002) interpreted Skouries to be an alkalic porphyry of shoshonitic affinity; however, petrographic evidence indicates K_2O enrichment may reflect intense potassic alteration. Frei (1995) also suggested that potassic alteration at Skouries resulted in a 20 to 36 relative percent increase in K_2O content. This study proposes a high K calc-alkaline classification for Skouries and its unaltered equivalent at Aspro Lakkos. A genetic relationship among both porphyry intrusions at Skouries and Aspro Lakkos is inferred based on petrography and geochemistry as originally proposed by Frei (1992). Lower K_2O contents of quartz-sericite-pyrite-altered porphyry dikes surrounding the Skouries stock are interpreted to be the result of alkali mobility during alteration and surface weathering (Fig. 10D).

Geochemical data from early Miocene dikes are plotted on the plutonic classification diagram of Middlemost (1994), albeit their texture is more characteristic of trachyandesite to trachydacite volcanic rocks (Fig. 10B). Glomerophyric porphyry dikes appear to be mildly alkalic to predominately subalkalic high K calc-alkaline with a tendency toward shoshonitic compositions. Quartz-sericite-carbonate-pyrite alteration is common among glomerophyric dikes, probably explaining the broad range of alkali contents. Unaltered samples from Piavitsa and Olympias drill core represent the least altered chemistry of these dikes (Fig. 10D). The unaltered black-matrix

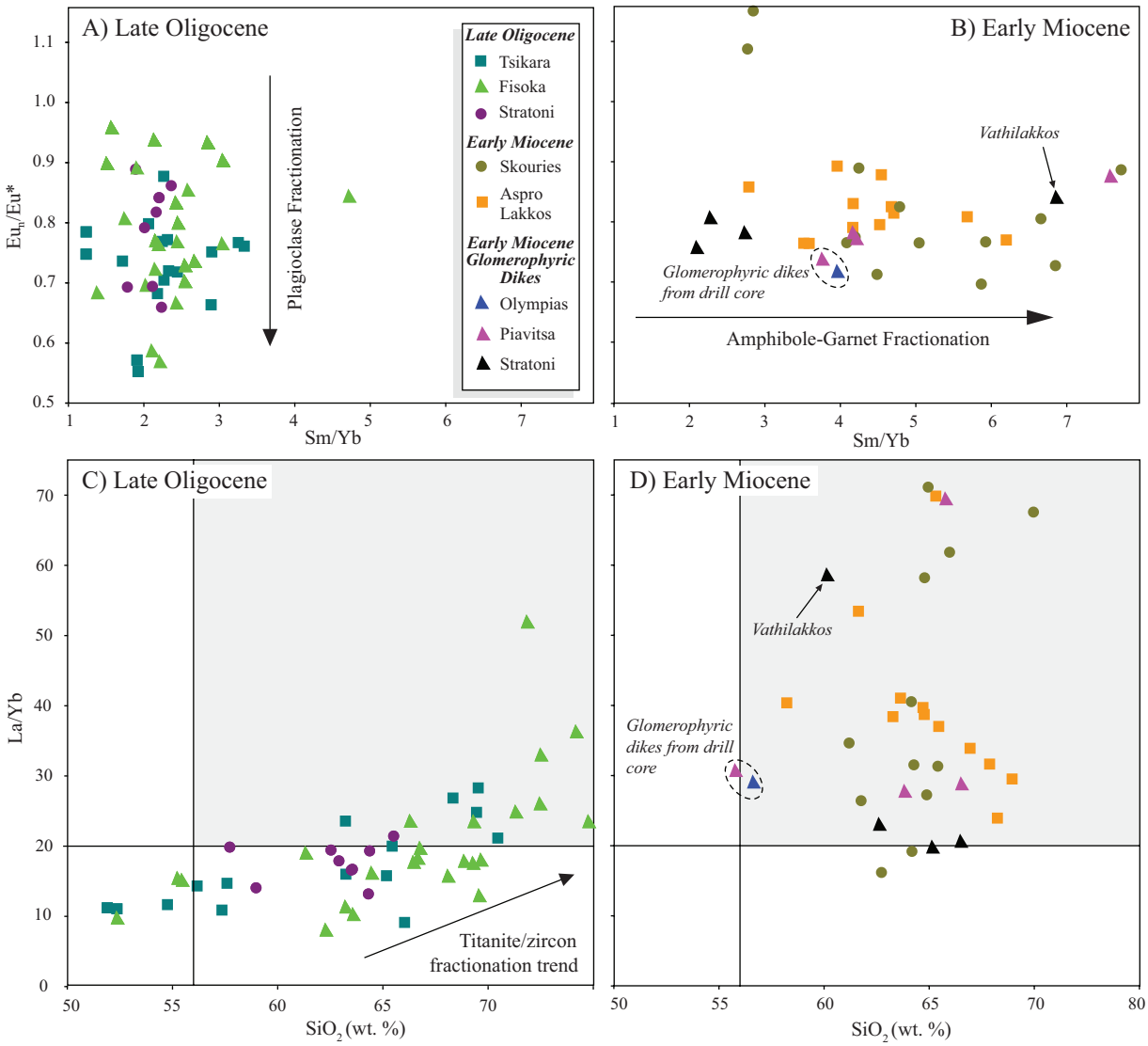

Fig. 12. Europium anomaly (Eu$_n$/Eu*) vs. Sm/Yb fractionation plots for (A) late Oligocene and (B) early Miocene igneous rocks. The europium anomaly is calculated using the equation in Rollinson (1993), and normalized relative to C1 chondrite values (Sun and McDonough, 1989). La/Yb vs. silica fractionation plots for the (C) late Oligocene and (D) early Miocene igneous suites. Shaded area represents the adakitic field of Richards and Kerrich (2007).

porphyry dike at Vathilakkos is high K calc-alkaline and contains similar alkali contents as the black-matrix porphyry dikes at Aspro Lakkos.

The early Miocene intrusive suite is more enriched in LREE but displays similar chondrite-normalized HREE patterns when compared against late Oligocene igneous rocks (Fig. 11D-F). However, late Miocene porphyritic stocks and dikes are distinctly HREE fractionated with Sm/Yb ratios of 2.77 to 7.72 at Skouries, 2.79 to 6.20 at Aspro Lakkos, and 6.87 from the black-matrix porphyry at Vathilakkos (Fig. 12B). Glomerophyric dikes have a wide range of Sm/Yb values (1.77–7.57; Fig. 12B). High average La/Yb and Sr/Y ratios occur at Skouries (43.42 and 83.6, respectively) and Aspro Lakkos (39.79 and 47.1, respectively; Fig. 12D). Weakly negative europium anomalies (Eu$_n$/Eu*) are evident at Aspro Lakkos (0.76–0.89) and Skouries (0.70–0.89) with two samples from the Skouries stock exhibiting slightly positive anomalies (1.08 and 1.15; Fig. 12B). The black-matrix porphyry dike at Vathilakkos and glomerophyric dikes display weak negative Eu$_n$/Eu* anomalies (0.72–0.87) and, combined with the HREE pattern, also suggest fractionation controlled by amphibole or garnet (Fig. 12B).

Early Miocene porphyries have highly enriched incompatible LILE contents compared to the late Oligocene suite. Sr concentrations exceed 1,570 ppm at Skouries and 1,446 ppm at Aspro Lakkos, while Ba concentrations reach 2,885 and 4,190 ppm for Skouries and Aspro Lakkos, respectively. Extremely high Sr values (3,835 ppm) occur within the unaltered glomerophyric dike at Olympias while Sr concentrations (1,515 ppm) for the black-matrix porphyry dike at Vathilakkos are similar to Aspro Lakkos. These extremely high Sr contents suggest little to no plagioclase fractionation in the parental magma (Richards et al., 2012). Early Miocene porphyries are strongly elevated in U and Th with highest concentrations at Skouries with 19 and 67 ppm, respectively, consistent with the

results from Kroll et al. (2002), suggesting significant crustal interaction.

Metallogenic Framework

The regional framework of the Serbo-Macedonian metallogenic province was strongly influenced by Eocene-Miocene extension and exhumation of the southern Rhodope core complex of northern Greece. Exhumation of the southern Rhodope core complex along the Kerdilion detachment fault (Brun and Sokoutis, 2007; Wüthrich, 2009) is postulated to be the regional tectonic process that triggered upper crustal magmatism and metallogenesis (Marchev et al., 2005; Eliopoulos and Kilias, 2011; Hahn et al., 2012; Kydonakis et al., 2014).

The penetrative ductile S_1 structural fabric within the Kerdilion unit was likely established during regional Cretaceous to Eocene ductile deformation (Kilias et al., 1999). Evidence for an early compressional thrust event in the Stratoni fault area may have been focused on this structural anisotropy associated with rheologically weak marbles (Haines, 1998). Thrust faulting is likely coeval with the development of subparallel district-scale F_3 folds. Eocene extensional tectonics and core complex exhumation may have been initiated at the Rhodope-bounding Kerdilion detachment fault (Brun and Sokoutis, 2007; Wüthrich, 2009; Kydonakis et al., 2014). Ductile to semibrittle extensional reactivation of the preexisting Stratoni thrust fault resulted in the development of a normal fault (Haines, 1998; Siron et al., 2014). Mineralized strands of semibrittle deformation within the Stratoni stock indicate that late Oligocene magmas were emplaced prior to or contemporaneous with extensional deformation within the Stratoni fault zone. The structural relationship between the Kerdilion detachment fault and the mineralized normal fault at Stratoni is unclear.

The NE-trending axis of Oligo-Miocene intrusive centers in the Kassandra mining district align with the midcrustal, northeast-elongated early Miocene Kavala pluton to the northeast of the Chalkidiki peninsula (Fig. 1; Dinter et al., 1995; Dinter, 1998). Synintrusion mylonitic fabrics and stretching lineations within the Kavala pluton indicate a NE-oriented principal axis of extension along the prominent NW-trending Symvolon shear zone (Fig. 1). This crustal-scale rupture developed prior to early Miocene and is believed to have localized syntectonic magmatism at Kavala (Dinter et al., 1995). Exhumation of the southern Rhodope core complex may have influenced ascent of magmas to shallow crustal levels, preferentially exploiting favorable oblique structural intersections between NE-trending transtensional faults (e.g., Vathilakkos strike-slip fault) and WNW-trending structures such as the antiform that hosts Skouries and the normal fault at Stratoni.

Magmatic evolution

Late Oligocene magmatism spanned ~2.5 m.y., with emplacement of the Tsikara composite stock at 27.0 Ma, followed by variably differentiated high K calc-alkaline diorite and granodiorite intrusions at Stratoni and Fisoka from 25.8 to 24.5 Ma. The high K calc-alkaline Skouries quartz monzonite porphyry was emplaced at 20.6 Ma with porphyry-style mineralization inferred to be the same age as the main intrusive phase (Fig. 5; Hahn et al., 2012). The altered, albeit barren, quartz monzonite porphyry at Aspro Lakkos crystallized at 19.7 Ma, coeval with the postmineral radial dikes at Skouries and the compositionally similar late porphyry phase in the Skouries stock. The barren black-matrix porphyry dike at Vathilakkos represents the latest stage of early Miocene magmatism in the district at 19.2 Ma.

Late Oligocene and early Miocene magmatism display distinct compositional differences, suggesting different magma sources and/or fractionation and mixing histories. $^{87}Sr/^{86}Sr$ ratios reported from the compositionally diverse Tsikara and Stratoni stocks (Frei, 1992) are consistent with a mafic mantle-derived parental magma potentially with some input from crustal sources. This is in contrast to the more uniform compositions of early Miocene porphyries, which may have been derived from a single or well-mixed source. Skouries and Aspro Lakkos have $^{87}Sr/^{86}Sr$ ratios typical of upper mantle or lower crustal sources (Frei, 1995).

The importance of plagioclase fractionation in the late Oligocene igneous suite is indicated by distinct negative europium anomalies and low Sm/Yb ratios (Figs. 11A-C, 12A). However, increasing La/Yb ratios with silica content could indicate fractionation of titanite or perhaps zircon among the most differentiated porphyry phases (Fig. 12C; Richards et al., 2012).

Petrochemical characteristics of the Miocene suite, including highly fractionated LREE, elevated incompatible LILE including Sr and Ba, and high field strength elements including U and Th, suggest involvement of subduction-enriched metabasaltic continental lithosphere (Pe-Piper and Piper, 2006; Pe-Piper et al., 2009). This suite exhibits elevated Sr/Y (>50), Sm/Yb and La/Yb ratios (Fig. 12B, D), indicating that these melts were controlled by fractionation of amphibole, in an amphibole ± garnet-bearing source (Richards and Kerrich, 2007; Richards et al., 2012; Lu et al., 2015), or achieved through assimilation of crustal material during ascent to shallow crustal levels (Richards and Kerrich, 2007; Richards, 2011). Chondrite-normalized REE patterns, particularly for Skouries (Fig. 11D), favor fractionation processes that involved amphibole. In order to achieve high Sr/Y and La/Yb ratios, sufficient water must be available to fractionate amphibole and suppress plagioclase in the deep crust or mantle (Richards and Kerrich, 2007; Richards, 2011). The minor to absent europium anomaly suggests oxidizing conditions and/or elevated water content, which will also quell plagioclase crystallization. Abundant amphibole and biotite phenocrysts in the early Miocene porphyries indicate high concentrations of magmatic water. Depletion in Nb, Ta, and Ti further support a hydrous mantle-derived magma (Pe-Piper and Piper, 2006).

The petrologic data document a major change in the physiochemical conditions between the late Oligocene and the early Miocene. Late Oligocene plutonic rocks may reflect the culmination of subduction-related magmatism prior to lithospheric delamination (and slab rollback), resulting in thermal melting of continental lithosphere. Melting of previous subduction-modified metabasaltic lithosphere would have generated progressively more alkalic (or shoshonitic) magmas in the early Miocene (Pe-Piper and Piper, 2006), possibly resulting in melts more favorable for generating porphyry Au-Cu deposits (Müller and Groves, 2000).

Metallogenesis

As currently known, porphyry Au-Cu mineralization is restricted to a small early Miocene high K calc-alkaline quartz monzonite porphyry at Skouries, although magmatism of the same age and type is widespread in the area. Skouries shows similarities to silica-saturated, shoshonitic, pencil-shaped porphyry bodies in the Ridgeway-Cadia and North Parkes districts of NSW, Australia (Wilson, 2003). The Skouries porphyry stock intruded a thick sequence of relatively unreactive quartz-rich feldspar-biotite gneiss close to the axis of a major WNW-trending antiform. These lithologic and structural features aided in efficient focusing of magmatic-hydrothermal fluids within a favorable depositional environment (e.g., Wilkinson, 2013). Magmatic-hydrothermal fluid was confined to the stock and immediately adjacent wall rock as dense arrays of stockwork, NE-trending sheeted veins, and disseminated Au-bearing Cu sulfide mineralization. Intersections between discrete district-wide NE-trending structures and fabrics developed in the axis of the regional antiform are postulated to be the principal structural control influencing the upper crustal emplacement and focus of the Skouries magmatic-hydrothermal system.

The brittle-ductile, extensional Stratoni fault zone hosts the Madem Lakkos and Mavres Petres polymetallic carbonate-hosted sulfide orebodies and cuts the late Oligocene (25.8–24.5 Ma) high K calc-alkaline granodiorite at Stratoni. High-temperature Cu-rich skarn occurs adjacent to the Stratoni granodiorite stock and related porphyry dikes, and grades westward into Au-Ag-Pb-Zn massive sulfide at Madem Lakkos, and variably arsenopyrite-rich base metal massive sulfide at Mavres Petres. Massive silica-manganese replacement bodies and epithermal-style silica-rhodochrosite veins at Piavitsa may reflect a continuum of hydrothermal mineralization westward for 12 km from a source region in the Stratoni area coincident with late Oligocene intrusions at Stratoni and Fisoka (Fig. 2). Zonation from skarn into proximal base metal massive sulfide and distal manganese replacement bodies is a characteristic pattern among intrusion-related, carbonate-hosted replacement systems (Megaw et al., 1988). Enrichment of Au is relatively unusual among these deposit types, albeit a distinguishing feature of the massive sulfide deposits in the Stratoni area and Olympias.

The precise timing of Au-Ag-Pb-Zn-Cu carbonate replacement mineralization within the Stratoni fault zone is uncertain but is constrained by structural and intrusive events. A maximum age of ~25 Ma is constrained by the Stratoni granodiorite stock which is cut by the Stratoni fault and exhibits alteration that may represent the eastern extent of the Madem Lakkos orebody. Skarn mineralization near the contact of the Stratoni stock and related porphyry dikes further suggest that mineralization in the Stratoni fault may be coeval with this igneous event; however, this evidence does not definitively link Madem Lakkos to the Stratoni stock. The minimum age for the marble-hosted mineralization is constrained by the 19.2 Ma black-matrix porphyry dike at Vathilakkos that crosscuts the Madem Lakkos orebody at depth (Nebel, 1989; Haines, 1998), and the 20.6 Ma glomerophyric porphyry dike that crosscuts siliceous-rhodochrosite carbonate replacement mineralization at Piavitsa. Based on these constraints, the orebodies in the Stratoni fault zone formed between 25 and 20 Ma. The spatially associated late Oligocene igneous rocks on the eastern end of the Stratoni fault support the older mineralization age. A late Oligocene age was also tentatively proposed by Gilg and Frei (1994) based on K-Ar geochronology.

The precise age of the Olympias deposit 8 km north of the Stratoni fault is not well constrained. Unaltered glomerophyric porphyry dikes in the Olympias area are geochemically and petrographically similar to those in the Stratoni fault, although no crosscutting relationships have been directly observed in the Olympias orebody. The arsenopyrite Re-Os age (26.1 Ma) of Hahn et al. (2012) suggests a minimum Oligo-Miocene age of mineralization at Olympias. Similarities among Olympias, Madem Lakkos, and Mavres Petres, particularly with respect to sulfide mineralogy and replacement textures, strongly suggest that Olympias is similar in age to the Stratoni orebodies, but no direct connection has been established between these deposits.

The close proximity of the Skouries Au-Cu porphyry and polymetallic Au-Ag-Pb-Zn-Cu carbonate-hosted replacement bodies suggests that a similar crustal plumbing system tapped deep fertile source regions and efficiently transported magmas and magmatic-hydrothermal fluids to shallow crustal levels. The nature of the resulting deposits reflects contrasting controls on the release and movement of ore-forming fluids and depositional mechanisms within the upper crust. The Kassandra mining district, therefore, demonstrates the importance of tectonic and magmatic processes working in concert with structures in the shallow environment to generate economic concentration of mineralization.

Conclusions

Multiple stages of ductile deformation structurally preconditioned the Kerdilion metamorphic basement in the southern Rhodope core complex. Eocene to Miocene exhumation of the southern Rhodope core complex along the Kerdilion detachment fault may have triggered regional magmatism and metallogenesis. Ductile compressional deformation resulted in district-scale folds and the development of the proto-Stratoni thrust fault. A regional northeast-southwest axis of extension led to ductile and semibrittle reactivation of the Stratoni normal fault in the late Oligocene. Structural intersections with a WNW-trending antiform at Skouries and the Stratoni fault likely influenced the upper crustal emplacement of Oligo-Miocene stocks and dikes and associated magmatic-hydrothermal systems.

Zircon U-Pb geochronology defines two distinct magmatic episodes previously recognized in the district (Frei, 1992). The late Oligocene igneous suite encompasses monzogabbro and granodiorites belonging to the 27 Ma composite stock at Tsikara and the 25.8 to 24.5 Ma diorite to granodiorite stocks at Stratoni and Fisoka. The early Miocene suite includes the 20.6 Ma (Hahn et al., 2012) mineralized quartz monzonite porphyry stock at Skouries and coeval glomerophyric dikes, followed by the 19.7 Ma barren porphyry at Aspro Lakkos. Magmatism concluded with the 19.2 Ma porphyry dike that intrudes the Vathilakkos fault. Both igneous suites belong to the high K calc-alkaline magmas series, with early Miocene porphyries showing a shoshonitic affinity. Fractionation patterns utilizing the Sm/Yb ratio and the Eu_n/Eu^* anomaly

indicate plagioclase control for the late Oligocene suite. In contrast, these ratios along with elevated Sr/Y and La/Yb values indicate fractionation of amphibole or garnet for the early Miocene suite of porphyries. Enriched LREE patterns, and extremely elevated LILE concentrations indicate that both magma suites, particularly the early Miocene porphyry event, interacted strongly with subduction-enriched continental lithosphere (Pe-Piper et al., 2006).

Two major mineralizing styles comprise the economic mineral deposits of the Kassandra mining district. Polymetallic Au-rich mineralization is hosted by marble contained within the semibrittle Stratoni fault. Mineralization is zoned along a 12-km strike length from Cu-bearing skarn adjacent to the late Oligocene Stratoni granodiorite stock, through Au-Ag-Pb-Zn-Cu carbonate replacement deposits at Madem Lakkos and Mavres Petres, to distal siliceous-manganese carbonate replacement bodies and associated crustiform Au-rich silica-rhodochrosite veins at Piavitsa. Structural and alteration relationships suggest that carbonate replacement mineralization is syn- to postemplacement of the late Oligocene Stratoni granodiorite stock (~25 Ma). Unaltered dikes at Vathilakkos and Piavitsa demonstrate that this mineralization predates early Miocene (19–20 Ma) magmatism. The Olympias Au-Ag-Pb-Zn carbonate replacement deposit is located 8 km north of the Stratoni fault. Olympias appears to be broadly similar to the Madem Lakkos and Mavres Petres deposits and the Re-Os age (26.1 Ma) of Hahn et al. (2012) suggests a similar timing. Early Miocene Au-Cu mineralization at Skouries, 8 km south of the Stratoni fault, is associated with a narrow pipe-shaped multiphase porphyry stock. Mineralization is hosted by multiple phases of porphyry-related quartz and quartz-magnetite veins associated with pervasive potassic alteration in the porphyry stock and adjacent wall-rock gneiss and schist.

Late Oligocene and early Miocene magmatism overlaps spatially within the district but defines distinct petrogenetic events separated by about 5 m.y. Both episodes are associated with Au-rich mineralization. Carbonate replacement deposits appear to have formed in association with high K calc-alkaline magmas, whereas the Skouries porphyry system has characteristics similar to subalkaline and shoshonitic porphyry deposits elsewhere. Carbonate replacement massive sulfide deposition was largely controlled by hydrothermal fluid movement into an extensional fault zone containing receptive host rocks, whereas a major regional fold axis localized the Skouries porphyry system. The change in character of mineralization within the Kassandra mining district may reflect a combination of factors, including structural preconditioning, magmatic-hydrothermal processes, and availability of reactive host rocks.

Acknowledgments

The first author would like to thank Eldorado Gold Corporation for providing logistical support while in Greece and financial support for analyses. CRS gratefully acknowledges the unwavering support from everyone at the Hellas Gold Exploration office at Madem Lakkos. Discussions among the authors with Dave Rhys and Peter Lewis contributed to the structural framework and interpretation. Samuel Haines is thanked for providing a copy of his thesis and discussing the evolution of the Stratoni fault from the now-closed Madem Lakkos mine. Geochronology support was provided by H. Lin and D. Newton (UBC). A travel grant was generously provided by the Mario Einaudi Center for International Studies at Cornell University. Critical reviews by Nikolay Bonev, Jeremy Richards, and an anonymous reviewer significantly improved this manuscript.

REFERENCES

Arvanitidis, N.D., and Constantinides, D.C., 1994, Ore geology of the Olympias, Madem Lakkos and Mavres Petres polymetallic deposits: Post-congress 2-day field trip to Chalkidiki peninsula (central Macedonia, northern Greece), Congress of the Geological Society of Greece, 7th, Thessaloniki, Greece, May 27–28, 1994, Guidebook, 17 p.

Barcikowski, J., Lehmann, S., von Quadt, A., Heinrich, C., and Serafimowski, T., 2012, The magmatic evolution of the Buchim-Damjan-Borov Dol ore district [abs.], *in* von Quadt, A., and Serafimovski, T., eds., Diversity of copper and gold deposits in the eastern European Balkan, Carpathian and Rhodopean belts: Tectonic, magmatic and geochronological investigations: SCOPES Project, International Conference, Stip, Macedonia, p. 16.

Bébien, J., Michard, A., Montigny, R., Feinberg, H., and Voidomatis, P., 2001, The Grigoriou plutonic complex (Mt. Athos, Greece): A component of the north Aegean Eocene-Oligocene calc-alkaline magmatism [abs.]: European Union of Geosciences Symposium, 11th, Strasbourg, France, 2001, LS03:314.

Bissig, T., and Tosdal, R.M., 2012, Petrogenetic and metallogenic relationships in the eastern Cordillera Occidental of central Peru: Journal of Geology, v. 117, p. 499–518.

Black, L.P., Kamo, S.L., Allen, C.M., Davis, D.W., Aleinikoff, J.N., Valley, J.W., Mundil, R., Campbell, I.H., Korsch, R.J., Williams, I.S., and Foudoulis, C., 2004, Improved Pb-206/U-218 microprobe geochronology by the monitoring of a trace-element-related matrix effect: SHRIMP, ID-TIMS, ELA-ICP-MS and oxygen isotope documentation for a series of zircon standards: Chemical Geology, v. 205, p. 115–140.

Bonev, N., and Dilek, Y., 2010, Geochemistry and tectonic significance of proto-ophiolitic metamafic units from the Serbo-Macedonian and western Rhodope massifs (Bulgaria-Greece): International Geology Review, v. 52, p. 298–335.

Bonev, N., Burg, J.-P., and Ivanov, Z., 2006, Mesozoic-Tertiary structural evolution of an extensional gneiss dome—the Kesebir-Kardamos dome, eastern Rhodope (Bulgaria-Greece): International Journal of Earth Science, v. 95, p. 318–340.

Bonev, N., Dilek, Y., Hanchar, J.M., Bogdanov, K., and Klain, L., 2012, Nd-Sr-Pb isotopic composition and mantle sources of Triassic rift units in the Serbo-Macedonian and western Rhodope massifs (Bulgaria-Greece): Geological Magazine, v. 149, p. 146–152.

Brun, J.P., and Sokoutis, D., 2007, Kinematics of the southern Rhodope core complex (north Greece): International Journal of Earth Science., v. 96, p. 1079–1099.

——2010, 45 m.y. of Aegean crust and mantle flow driven by trench retreat: Geology, v. 38, p. 815–818.

Burg, J.-P., Ivanov, Z., Ricou, L.-E., Dimor, D., and Klain, L., 1990, Implications of shear-sense criteria for the tectonic evolution of the Central Rhodope massif, southern Bulgaria: Geology, v. 18, p. 451–454.

Burg, J.-P., Ricou, L.-E., Ivanov, Z., Godfriaux, I., Dimov, D., and Klain, L., 1993, Crustal-scale thrust complex in the Rhodope. Structure and kinematics: Bulletin of the Geological Society of Greece, v. 29, p. 71–85.

——1996, Syn-metamorphic nappe complex in the Rhodope massif: Structure and kinematics: Terra Nova, v. 8, p. 6–15.

Burgath, K., Kockel, F., Mohr, F., Raschka, H., Jung, D., and Mussalam, K., 1980, A complex of sheeted dykes and pillow lavas in the southern part of the Chalkidiki peninsula, Greece [ext. abs.]: International Ophiolite Symposium, 2nd, Nicosia, Cyprus, 1980, Extended Abstracts, p. 20.

Christofides, G., D'Amico, C., Del Moro, A., Eleftheriadis, G., and Kyriakopoulos, C., 1990, Rb-Sr-geochronology and geochemical characters of the Sithonia plutonic complex (Greece): European Journal of Mineralogy, v. 2, p. 79–87.

Christofides, G., Koroneos, A., Liati, A., and Kral, J., 2007, The A-type Kerkini granitic complex in north Greece: Geochronology and geodynamic implications: Bulletin of the Geological Society of Greece, v. 40, p. 700–711.

de Boorder, H., Spakman, W., White, S.H., and Wortel, M.J.R., 1998, Late Cenozoic mineralization, orogenic collapse and slab detachment in the European Alpine belt: Earth and Planetary Letters, v. 164, p. 569–575.

De Wet, A.P., Miller, J.A., Bickle, M.J., and Chapman, H.J., 1989, Geology and geochronology of the Arnea, Sithonia and Ouranoupolis intrusions, Chalkidiki peninsula, northern Greece: Tectonophysics, v. 161, p. 65–79.

Dimitriadis, S., Kondopoulou, D., and Atzemoglou, A., 1998, Dextral rotations and tectonomagmatic evolution of the southern Rhodope and adjacent regions (Greece): Tectonophysics, v. 299, p. 159–173.

Dinter, D.A., 1998, Late Cenozoic extension of the Alpine collisional orogen, northeastern Greece: Origin of the north Aegean basin: Geological Society of America Bulletin, v. 110, p. 1208–1230.

Dinter, D.A., Macfarlane, A., Hames, W., Isachsen, C., Bowring, S., and Royden, L., 1995, U-Pb and $^{40}Ar/^{39}Ar$ geochronology of the Symvolon granodiorite: Implications for the thermal and structural evolution of the Rhodope metamorphic core complex, northeastern Greece: Tectonics, v. 14, p. 886–908.

Diodorus Siculus, Library of history volume VIII, books 16.66–17, Welles, B.C., trans., Loeb Classical Library 422: Cambridge, MA, Harvard University Press, 1963.

Dixon, J.E., and Dimitriadis, S., 1984, Metamorphosed ophiolitic rocks from the Serbo-Macedonian massif near lake Volvi, north-east Greece: Geological Society of London Special Publication 17, p. 603–618.

Dragić, D., Mišković, A., Hart, C., Tosdal, R., Dunav, P.F., and Glisic, S., 2014, Spatial and temporal relations between epithermal and porphyry style mineralization in the Lece magmatic complex, Serbia [ext. abs.]: Society of Economic Geologists 2014 Conference: Building Exploration Capability for the 21st Century, Keystone, Colorado, 2014, Extended Abstracts.

Eldorado Gold Corporation, 2016, Resources and reserves: Accessed February 22, 2016, (http://www.eldoradogold.com/assets/resources-and-reserves/).

Eliopoulos, D.G., and Economou-Eliopoulos, M., 1991, Platinum-group elements and gold contents in the Skouries porphyry copper deposit, Chalkidiki peninsula, northern Greece: Economic Geology, v. 86, p. 740–749.

Eliopoulos, D., and Kilias, S.P., 2011, Marble-hosted submicroscopic gold mineralization at Asimotrypes area, Mount Pangeon, southern Rhodope core complex, Greece: Economic Geology, v. 106, p. 751–780.

Eliopoulos, D.G., Economou-Eliopoulos, M., and Zelyaskova-Panayiotova, M., 2014, Critical factors controlling Pd and Pt potential in porphyry Cu-Au deposits: Evidence from the Balkan Peninsula: Geosciences, v. 4, p. 31–49.

Forward, P., Francis, A., and Liddell, N., 2010, Technical report on the Stratoni project Pb-Zn-Ag deposit, northern Greece: European Goldfields Limited, Report NI 43-101, 54 p.

Frei, R., 1992, Isotope (Pb-Rb-Sr-S-O-C-U-Pb) geochemical investigations of Tertiary intrusions and related mineralizations in the Serbo-Macedonian (Pb-Zn, Sb + Cu-Mo metallogenetic) province in northern Greece: Ph.D. thesis, Zürich, Switzerland, ETH, 231 p.

——1995, Evolution of mineralizing fluid in the porphyry copper system of the Skouries deposit, northeast Chalkidiki (Greece): Evidence from combined Pb-Sr and stable isotope data: Economic Geology, v. 90, p. 746–762.

——1996, The extent of inner mineral isotope equilibrium: A systematic bulk U-Pb and Pb step leaching (PbSL) isotope study of individual minerals from the Tertiary granite of Jerissos (northern Greece): European Journal of Mineralogy, v. 8, p. 1175–1189.

Fytikas, M., Innocenti, F., Manetti, P., Mazzuoli, R., Peccerillo, A., and Villari, L., 1984, Tertiary to Quaternary evolution of volcanism in the Aegean region: Geological Society of London Special Publication 17, p. 687–699.

Gautier, P., Brun, J.-P., Moriceau, R., Sokoutis, D., Martinod, J., and Jolivet, L., 1999, Timing, kinematic and cause of Aegean extension: A scenario based on a comparison with simple analogue experiments: Tectonophysics, v. 315, p. 31–72.

Gilg, H.A., 1993, Geochronology (K-Ar), fluid inclusion, and stable isotope (C, H, O) studies of skarn, porphyry copper, and carbonate-hosted Pb-Zn (Ag, Au) replacement deposits in the Kassandra mining district (eastern Chalkidiki, Greece): Ph.D. thesis, Zürich, Switzerland, ETH, 153 p.

Gilg, H.A., and Frei, R., 1994, Chronology of magmatism and mineralization in the Kassandra mining area, Greece: The potentials and limitations of dating hydrothermal illites: Geochimica et Cosmochimica Acta, v. 58, p. 2107–2122.

Gilg, H.A., Frei, R., Kalogeropoulos, S.I., and Nicolaou, M., 1992, Metamorphism and polygenesis of the Madem Lakkos polymetallic sulfide deposit, Chalkidiki, Greece—a discussion: Economic Geology, v. 87, p. 1184–1193.

Hahn, A., Naden, J., Treloar, P.J., Kilias, S.P., Rankin, A.H., and Forward, P., 2012, A new time frame for the mineralization in the Kassandra mine district, N Greece: Deposit formation during metamorphic core complex exhumation: European Mineralogical Conference, v. 1, 1EMC2012-742.

Haines, H.S., 1998, A structural synthesis for sector Vb of the Madem Lakkos polymetallic sulfide deposit—northeast Greece: M.Sc. thesis, London, United Kingdom, University of London, 81 p.

Hanson, G., 1980, Rare earth elements in petrogenetic studies of igneous systems: Annual Review of Earth and Planetary Sciences, v. 8, p. 371–406.

Heinrich, C.A., and Neubauer, F., 2002, Cu-Au-Pb-Zn-Ag metallogeny of the Alpine-Balkan-Carpathian-Dinaride geodynamic province: Mineralium Deposita, v. 37, p. 533–540.

Himmerkus, F., Zachariadis, P., Reischmann, T., and Kostopoulos, D.K., 2005, The mafic complexes of the Athos-Volvi-zone—a suture zone between the Serbo-Macedonian massif and the Rhodope massif? [abs.]: Geophysical Research Abstracts, v. 7, p. 10, 240.

Himmerkus, F., Reischmann, T., and Kostopoulos, D.K., 2006, Late Proterozoic and Silurian basement units within the Serbo-Macedonian massif, northern Greece: the significance of terrane accretion in the Hellenides: Geological Society of London Special Publication 260, p. 35–50.

Himmerkus, F., Anders, B., Reischmann, T., and Kostopoulos, D., 2007, Gondwana-derived terranes in the northern Hellenides: Geological Society of America Memoir, v. 200, p. 379–390.

Himmerkus, F., Reischmann, T., and Kostopoulos, D.K., 2009a, Serbo-Macedonian revisited: A Silurian basement terrane from northern Gondwana in the Internal Hellenides, Greece: Tectonophysics v. 473, p. 20–35.

——2009b, Triassic rift-related meta-granites in the Internal Hellenides, Greece: Geological Magazine, v. 146, p. 252–265.

Himmerkus, F., Zachariadis, P., Reischmann, T., and Kostopoulos, D., 2011, The basement of the Mount Athos Peninsula, northern Greece: Insights from geochemistry and zircon ages: International Journal of Earth Science, v. 101, p. 1467–1485.

Irvine, T.N., and Baragar, W.R.A., 1971, A guide to the chemical classification of the common volcanic rocks: Canadian Journal of Earth Science, v. 8, p. 523–548.

Janković, S., 1997, The Carpatho-Balkanides and adjacent area: A sector of the Tethyan Eurasian metallogenic belt: Mineralium Deposita, v. 32, p. 426–433.

Jolivet, L., Faccenna, C., Huet, B. , Labrousse, L., Le Pourhiet, L., Lacombe, O., Lecomte, E, Burov, E, Denele, Y., Brun, J.P., Philippon, M., Paul, A., Salaun, G., Karabulut, H., Piromallo, C., Monie, P., Gueydan, F., Okay, A.I., Oberhansli, R., Pourteau, A., Augier, R., Gadenne, L, and Driussi, O., 2013, Aegean tectonics: Strain localization, slab tearing and trench retreat: Tectonophysics, v. 597–598, p. 1–33.

Jones, C.E., Tarney, J., Baker, J.H., and Gerouki, F., 1992, Tertiary granitoids of Rhodope, northern Greece: Magmatism related to extensional collapse of the Hellenic orogen?: Tectonophysics, v. 210, p. 295–314.

Kalogeropoulos, S.I., Economou, G.S., Gerouki, F., Karamonou, E., Kougoulis, C., and Perlikos, P., 1989a, The mineralogy and geochemistry of the Stratoni granodiorite and its metallogenetic significance: Bulletin of the Geological Society of Greece, v. 25, p. 225–243.

Kalogeropoulos, S.I., Kilias, S.P., Bitzios, D.C., Nicolaou, M., and Both, R.A., 1989b, Genesis of the Olympias carbonate-hosted Pb-Zn (Au, Ag) sulfide ore deposit, eastern Chalkidiki peninsula, northern Greece: Economic Geology, v. 84, p. 1210–1234.

Kalogeropoulos, S.I., Frei, R., Nikolaou, M., and Gerouki, F., 1990, Origin and metallogenetic significance of the Tertiary Stratoni granodiorite, Chalkidiki, N. Greece: Isotope and chemical evidence: Bulletin of the Geological Society of Greece, v. 26, p. 23–38.

Kalogeropoulos, S.I., Gerouki, F., and Papadopoulos, C., 1991, Mineralogy-geochemistry-genesis and metallogenetic significance of lamprophyres from the Stratoni-Olympias area Kerdilia formation, eastern Chalkidiki: Bulletin of the Geological Society of Greece, v. 27, p. 161–173.

Kay, S.M., and Mpodozis, C., 2001, Central Andean ore deposits linked to evolving shallow subduction systems and thickening crust: GSA Today, v. 11, no. 3, p. 4–9.

Kilias, A., Falalakis, G., and Mountrakis, D., 1999, Cretaceous-Tertiary structures and kinematics of the Serbomacedonian metamorphic rocks and their relation to the exhumation of the Hellenic hinterland (Macedonia, Greece): International Journal of Earth Sciences, v. 88, p. 513–531.

Kilias, S.P., Kalogeropoulos, S.I., and Konnerup-Madsen, J., 1996, Fluid inclusion evidence for the physicochemical conditions of sulfide deposition in the Olympias carbonate-hosted Pb-Zn(Au, Ag) sulfide ore deposit, E. Chalkidiki peninsula, N. Greece: Mineralium Deposita, v. 31, p. 394–406.

Kockel, F., Mollat, H., and Gundlach, H., 1975, Hydrothermally altered and (copper-) mineralized porphyritic intrusions in the Serbo-Macedonian massif (Greece): Mineralium Deposita, v. 10, p. 195–204.

Kockel, F., Mollat, H., and Walther, H., 1977, Erläuterungen yur geologischen karte der Chalkidiki und agrenzender Gebiete 1:100000 (Nord-Griechenland): Bundesanstalt für Geowissenschaften Rohstoffe, Hannover, p. 1–119.

Krenn, K., Bauer, C., Proyer, A., Klözli, U., and Hoinkes, G., 2010, Tectonometamorphic evolution of the Rhodope orogen: Tectonics, v. 29, TC4001.

Kroll, T., Müller, D., Seifert, T., Herzig, P.M., and Schneider, A., 2002, Petrology and geochemistry of the shoshonite-hosted Skouries porphyry Cu-Au deposit, Chalkidiki, Greece: Mineralium Deposita, v. 37, p. 137–144.

Kydonakis, K., Gallagher, K., Brun, J.-P., Jolivet, M., Gueydan, F., and Kostopoulos, D., 2014, Upper Cretaceous exhumation of the western Rhodope metamorphic province (Chalkidiki peninsula, northern Greece): Tectonics, v. 33, p. 1113–1132.

Lips, A.L., 2002, Correlating magmatic-hydrothermal ore deposit formation over time with geodynamic processes in SE Europe: Geological Society of London Special Publication 204, p. 69–79.

Lips, A.L.W., White, S.H., and Wijbransb, J.R., 2000, Middle-Late Alpine thermotectonic evolution of the southern Rhodope massif, Greece: Geodinamica Acta, v. 13, p. 281–292.

Lu, J.Y., Loucks, R.R., Fiorentini, M.L., Yang, Z.M., and Hou, Z.Q., 2015, Fluid flux melting generated postcollisional high Sr/Y copper ore-forming water-rich magmas in Tibet: Geology, v. 43, p. 583–586.

Ludwig, K.R., 2003, Isoplot 3.09—a geochronological toolkit for Microsoft Excel: Berkeley Geochronology Center, Special Publication 4.

Marchev, P., Kaiser-Rohrmeier, M., Heinrich, C., Ovtcharova, M., von Quadt, A., and Raicheva, R., 2005, 2: Hydrothermal ore deposits related to post-orogenic extensional magmatism and core complex formation: the Rhodope massif of Bulgaria and Greece: Ore Geology Reviews, v. 27, p. 53–89.

McFall, K.A., Roberts, S., Teagle, D., Naden, J., Lusty, P., and Boyce, A., 2016, The origin and distribution of critical metals (Pd, Pt, Te & Se) within the Skouries Cu-Au porphyry deposit, Greece [ext. abs.]: Mineral Deposits Study Group Meeting, 39th, Dublin, Ireland, 2016, Extended Abstracts.

Megaw, P.K.M., Ruiz, J., and Titley, S.R., 1988, High-temperature, carbonate-hosted Ag-Pb-Zn(Cu) deposits of northern Mexico: Economic Geology, v. 83, p. 1856–1885.

Middlemost, E.A.K., 1994, Naming materials in the magma/igneous rock system: Earth-Science Reviews, v. 37, p. 215–224.

Müller, D., and Groves, D.L., 2000, Potassic igneous rocks and associated gold-copper mineralization: New York, Springer, 252 p.

Nebel, M.L., 1989, Metamorphism and polygenesis of the Madem Lakkos polymetallic sulfide deposit, Chalkidiki, Greece: Ph.D. thesis, Golden, Colorado, Colorado School of Mines, 215 p.

Nebel, M.L., Hutchinson, R.W., and Zartman, R.E., 1991, Metamorphism and polygenesis of the Madem Lakkos polymetallic sulfide deposit, Chalkidiki, Greece: Economic Geology, v. 86, p. 81–105.

Neubauer, F., 2002, Contrasting Late Cretaceous with Neogene ore provinces in the Alipine-Balkan-Carpathian-Dinaride collision belt: Geological Society of London Special Publication 204, p. 81–102.

Neubauer, W.H., 1957, Geologie der blei-zink reichen kieslagerstätten von Kassandra (Chalkidike, Griechenland): Berg- und Hüttenmännische Monatshefte, v. 102, p. 1–16.

Nicolaou, M.N., 1960, L'intrusion granitique dans la région de Stratoni-Olympiade et sa relation avec la métallogenèse: Annales Géologiques des Pays Helléniques, v. 11, p. 214–265.

——1964, The mineralogy and micrography of the sulphide ores of Kassandra mines, Greece: Annales Géologiques des Pays Helléniques, v. 16, p. 111–139.

——1969, Recent research on the composition of the Kassandra mines orebodies: Praktika tes Academias Athenon, v. 44, p. 82–93 (in Greek with English abs.).

Papadakis, A., 1971, On the age of the granitic intrusions near Stratonion Chalkidiki, Greece: Annales Géologiques des Pays Helléniques, v. 23, p. 297–300.

Papanikolaou, D., 2013, Tectonostratigraphic models of the Alpine terranes and subduction history of the Hellenides: Tectonophysics, v. 595–596, p. 1–24.

Paton, C., Hellstrom, J., Paul, B., Woodhead, J., and Hergt, J., 2011, Iolite: Freeware for the visualization and processing of mass spectrometric data: Journal of Analytical Atomic Spectrometry, v. 26, p. 2508–2518.

Pavlides, S.B., and Tranos, M.D., 1991, Structural characteristics of two strong earthquakes in the north Aegean: Ierissos (1932) and Agios Efstratios (1968): Journal of Structural Geology, v. 13, p. 205–214.

Pe-Piper, G., and Piper, D.J.W., 2002, The igneous rocks of Greece: Stuttgart, Borntraeger, 645 p.

——2006, Unique features of the Cenozoic igneous rocks of Greece: Geological Society of America Special Paper 409, p. 259–282.

Pe-Piper, G., Piper, D.J.W., Koukouvelas, I., Dolansky, L.M., and Kokkalas, S., 2009, Postorogenic shoshonitic rocks and their origins by melting underplated basalts: The Miocene of Limnos, Greece: Geological Society of America Bulletin, v. 121, p. 39–54.

Piercey, S.J., 2014, A review of quality assurance and quality control (QA/QC) procedures for lithogeochemical data: Geoscience Canada, v. 41, p. 75–88.

Richards, J.P., 2011, High Sr/Y arc magmas and porphyry Cu ± Mo ± Au deposits: Just add water: Economic Geology, v. 106, p. 1075–1081.

Richards, J.P., and Kerrich, R., 2007, Adakite-like rocks: Their diverse origins and questionable role in metallogenesis: Economic Geology, v. 102, p. 537–576.

Richards, J.P., Spell, T., Rameh, E., Razique, A., and Fletcher, T., 2012, High Sr/Y magmas reflect arc maturity, high magmatic water content, and porphyry Cu ± Mo ± Au potential: Examples from the Tethyan arcs of central and eastern Iran and western Pakistan: Economic Geology, v. 107, p. 295–332.

Rickwood, P.C., 1989, Boundary lines within petrologic diagrams which use oxides of major and minor elements: Lithos, v. 22, p. 247–263.

Ricou, L.E., Burg, J.-P., Godfriaux, I., and Ivanov, Z., 1998, Rhodope and Vardar: the metamorphic and the olistostromic paired belts related to the Cretaceous subduction under Europe: Geodinamica Acta, v. 11, p. 285–309.

Ring, U., Glodny, J., Will, T., and Thomson, S., 2010, The Hellenic subduction system: High-pressure metamorphism, exhumation, normal faulting, and large-scale extension: Annual Reviews of Earth and Planetary Sciences, v. 38, p. 45–76.

Rock, N.M.S., 1991, Lamprophyres: Glasgow, Blackie, 285 p.

Rollinson, H. R., 1993, Using geochemical data: Evaluation, presentation, interpretation: London, Longman, 352 p.

Rudnick, R.L., and Gao, S., 2003, Composition of the continental crust: Treatise on Geochemistry, v. 3, p. 1–64.

Serafimovski, T., 2000, The Lece-Chalkidiki metallogenic zone: Geotectonic setting and metallogenic features: Geologija, v. 42, p. 159–164.

Serafimovski, T., Stefanova, V., and Volkov, A.V., 2010, Dwarf copper-gold porphyry deposits of the Buchim-Damjan-Borov Dol ore district, Republic of Macedonia (FYROM): Geology of Ore Deposits, v. 52, p. 179–195.

Sláma, J., Košler, J., Condon, D.J., Crowley, J.L., Gerdes, A., Hanchar, J.M., Horstwood, M.S.A., Morris, G.A., Nasdala, L., Norberg, N., Schaltegger, U., Schoene, B., Tubrett, M.N., and Whitehouse, M.J., 2008, Plesovice zircon—a new natural reference material for U-Pb and Hf isotopic microanalysis: Chemical Geology, v. 249, p. 1–35.

Siron, C.R., Thompson, J.F.H., Rhys, D., and Baker, T., 2014, Structural framework of Au-rich porphyry and carbonate-hosted replacement deposits of the Kassandra mining district, northern Greece [ext. abs.]: Society of Economic Geologists 2014 Conference: Building Exploration Capability for the 21st Century, Keystone, Colorado, 2014, Extended Abstracts.

Stefanova, E., Donkova, A., Georgiev, S., Marchev, P., and Waelle, M., 2012, Llovitsa porphyry Cu-Au deposit: Sequence of vein formation and sulfide deposition [abs.], *in* von Quadt, A., and Serafimovski, T., eds., Diversity of copper and gold deposits in the eastern European Balkan, Carpathian and Rhodopean belts: Tectonic, magmatic and geochronological investigations: SCOPES Project, International Conference, Stip, Macedonia, p. 16.

Strmić Palinkaš, S., Palinkaš, L.A., Renac, C., Spangenberg, J.E., Lüders, V., Moldar, F., and Maliqi, G., 2013, Metallogenic model of the Trepča Pb-Zn-Ag skarn deposit, Kosovo: Evidence from fluid inclusions, rare earth elements, and stable isotope data: Economic Geology, v. 108, p. 135–162.

Sun, S.S., and McDonough, W.F., 1989, Chemical and isotopic systematics of oceanic basalts: Implications for mantle composition and processes: Geological Society of London Special Publication 42, p. 313–345.

Tafti, R., Mortensen, J.K., Lang, J.R., Rebagliati, and Oliver, J.L., 2009, Jurassic U-Pb and Re-Os ages for the newly discovered Xietongmen Cu-Au porphyry district, Tibet, PRC: Implications for metallogenic epochs in the southern Gangdese belt: Economic Geology, v. 104, p. 127–136.

Thompson, T.B., and Arehart, G.B., 1990, Geology and the origin of ore deposits in the Leadville district, Colorado: Part I. Geologic studies of orebodies and wall rocks: Economic Geology Monograph 7, p. 130–155.

Tobey, E., Schneider, A., Algería, A., Olcay, L., Perantonis, G., and Quiroga, J., 1998, Skouries porphyry copper-gold deposit, Chalkidiki, Greece: Setting, mineralization and resources, in Porter, T.M., ed., Porphyry and hydrothermal copper and gold deposits: A global perspective: Adelaide, PGC Publishing, p. 175–184.

Tompouloglou, C., 1981, Les minéralisations tertiares, type cuivre porphyrique, du massif Serbo-Macédonien (Macédoine, Grèce) dans leur contexte magmatique (avec un traitment géostatistique pour les données du prospect d'Alexia): Ph.D. thesis, Paris, France, École Nationale Supérieure des Mines de Paris, 204 p.

Turpaud P., and Reischmann, T., 2003, Zircon ages of granitic gneisses from the Rhodope (N. Greece), determination of basement age evidences for a Cretaceous intrusive event [abs.]: Geophysical Research Abstracts, 5:04435.

Wawrzenitz, N., and Krohe, A., 1998, Exhumation and doming of the Thassos metamorphic core complex (S Rhodope, Greece): Structural and geochronological constrains: Tectonophysics, v. 285, p. 301–312.

Wilkinson, J.J., 2013, Triggers for the formation of porphyry ore deposits in magmatic arcs: Nature Geoscience, v. 6, p. 917–925.

Wilson, A.J., 2003, The geology, genesis and exploration context of the Cadia gold-copper porphyry deposits, NSW, Australia: Ph.D. thesis, Hobart, University of Tasmania, 335 p.

Wortel, M.J.R., and Spakman, W., 2000, Subduction and slab detachment in the Mediterranean-Carpathian region: Science, v. 290, p. 1910–1917.

Wüthrich, E., 2009, Low temperature thermochronology of the northern Aegean Rhodope massif: Ph.D. thesis, Zürich, Switzerland, ETH, 210 p.

Zachos, K., 1963, Discovery of a copper deposit in Chalkidiki peninsula, N-Greece: Geological and Geophysical Research, v. 8, p. 1–26.